111-24
201255
41 P

NASA TECHNICAL MEMORANDUM 109047

Time Dependent Behavior of a Graphite/Thermoplastic Composite and the Effects of Stress and Physical Aging

Thomas S. Gates and Mark Feldman

November 1993

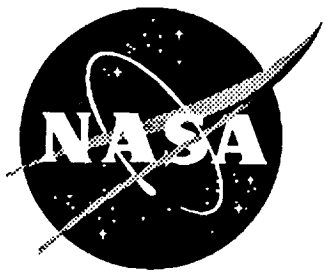

National Aeronautics and
Space Administration

LANGLEY RESEARCH CENTER
Hampton, Virginia 23681-0001

TIME DEPENDENT BEHAVIOR OF A GRAPHITE/THERMOPLASTIC COMPOSITE AND THE EFFECTS OF STRESS AND PHYSICAL AGING

Thomas S. Gates
NASA Langley Research Center
Hampton, Virginia

Mark Feldman
Old Dominion University
Norfolk, Virginia

ABSTRACT

Two complimentary studies were performed to determine the effects of stress and physical aging on the matrix dominated time dependent properties of IM7/8320 composite. The first of these studies, experimental in nature, used isothermal tensile creep/aging test techniques developed for polymers and adapted them for testing of the composite material. From these tests, the time dependent transverse (S_{22}) and shear (S_{66}) compliance's for an orthotropic plate were found from short term creep compliance measurements at constant, sub-T_g temperatures. These compliance terms were shown to be affected by physical aging. Aging time shift factors and shift rates were found to be a function of temperature and applied stress.

The second part of the study relied upon isothermal uniaxial tension tests of IM7/8320 to determine the effects of physical aging on the nonlinear material behavior at elevated temperature. An elastic/viscoplastic constitutive model was used to quantify the effects of aging on the rate-independent plastic and rate-dependent viscoplastic response. Sensitivity of the material constants required by the model to aging time were determined for aging times up to 65 hours. Verification of the analytical model indicated that the effects of prior aging on the nonlinear stress/strain/time data of matrix dominated laminates can be predicted.

INTRODUCTION

Design and trade studies are currently under way in the commercial aircraft industry to assess the materials and structures required for the development of the next generation, supersonic transport. This vehicle, designated the High Speed Civil Transport (HSCT) and targeted to carry over 300 passengers

at speeds in excess of mach 2, will have a useful lifetime of over 60,000 flight hours. During a typical flight skin temperatures may reach up to 400°F. To meet the weight requirements imposed by such design criteria, polymer matrix composite (PMC) materials are being considered for both primary and secondary structures.

One potential difficulty associated with using PMC's in such a vehicle is the task of predicting the changes in material properties due to aging of the PMC after long term exposure at temperature. These changes in the composite's strength and stiffness will be primarily due to changes in the mechanical properties of the matrix material. The aging of a polymer matrix may be due to some combination of physical aging, chemical aging and damage accumulation. It is the intent of this report to consider the effects due to just the physical aging process. This type of aging, considered to be a thermoreversible process, will cause changes in mechanical properties brought about by the volume recovery in the polymer upon cooling from above the glass transition (T_g) temperature. During aging, the polymer moves towards a state of equilibrium. This state of equilibrium, defined as the point of minimum volume change, is approached asymptotically.

Physical aging in polymers is a well-known phenomenon. Struik [1] performed one of the most comprehensive studies of physical aging. In his work he conducted numerous studies on the effects of load and environment on the physical aging of a variety of polymer systems. More recently, Sullivan [2], and Hastie and Morris [3], used experimental techniques established for polymers and extended them to study physical aging in glass/epoxy and graphite/thermoplastic continuous fiber PMC's. Their studies concentrated on using momentary creep tests to determine the principal compliance terms and aging shift rates for a laminated composite as a function of temperature and aging time. Testing was performed isothermally and within the linear viscoelastic range. Results from this work showed that physical aging directly influenced the short and long term creep compliance. In other work, Chen et.al [4] studied the effects of aging on the toughness of graphite/thermoplastic, continuous fiber PMC's. Chen found that parameters such as Mode I strain energy release rate, damage initiation force and propagation energy decreased with increases in the aging temperature and time.

The objectives of this research were twofold. The first was to experimentally measure short term, elevated temperature creep compliance in IM7/8320, a graphite/thermoplastic, and determine the effects of stress and physical aging on the matrix dominated compliance. The second objective was to determine how physical aging affects the nonlinear stress/strain behavior at elevated temperature. An elastic/viscoplastic constitutive model was used to quantify the effects of aging on the rate-independent plastic and rate-dependent viscoplastic response. These studies may provide a source of durability analysis tools and accelerated test methods for HSCT materials development.

TENSILE CREEP COMPLIANCE

The first study undertaken centered on using momentary creep compliance tests to determine the aging behavior of the principal compliance terms for a laminated composite as a function of stress and temperature. Using a three parameter model of creep compliance, aging shift factors and shift rates were investigated for three temperatures below the T_g. Isothermal, elevated temperature creep tests provided the short term creep compliance data. To establish stress levels for the aging tests, short term,

isothermal creep tests were run at increasingly higher stresses. In addition, creep/recovery tests provided insights into the effects of short versus long recovery periods and the applicability of Boltzman's superposition principle [5]. Other tests looked at the effects of stress on creep compliance while aging to equilibrium.

Analytical Models

The analytical modeling provided a means of describing changes due to physical aging in creep compliance of a laminated plate. For the laminates in this study, the usual axes' definitions for an orthotropic plate were used, e.g., 1= along the fiber, 2= transverse to the fiber, x= axial loading direction, y= transverse to loading direction, and the angle between the 1,2 axes and the x,y axes was measured clockwise.

The general case of a thin orthotropic plate was considered. For a state of plane stress parallel to the x-y plane in an orthotropic solid, the constitutive relation can be given by

$$\begin{Bmatrix} \varepsilon_{11} \\ \varepsilon_{22} \\ \gamma_{12} \end{Bmatrix} = \begin{bmatrix} S_{11} & S_{12} & 0 \\ S_{21} & S_{22} & 0 \\ 0 & 0 & S_{66} \end{bmatrix} \begin{Bmatrix} \sigma_{11} \\ \sigma_{22} \\ \sigma_{12} \end{Bmatrix} \tag{1}$$

Where ε and γ are the strains, S_{ij} is the compliance, and σ is the stress.

This set of equations implies that there are four independent constants needed to characterize the material. These constants are the longitudinal and transverse compliance, S_{11} and S_{22} respectively, Poison's ratio υ_{12}, and the shear compliance S_{66}. A primary assumption was that physical aging occurred only in the polymer matrix constituent. On the basis of tests performed by Sullivan[2] and Hastie and Morris[3], an assumption was that S_{22} and S_{66} were the two compliance terms to be affected by physical aging.

Creep tests allowed an assessment of the time-dependent compliance changes in both the S_{22} and S_{66} terms. These tests were analyzed using linear viscoelastic theory and standard[1] sub-T_g creep/aging data reduction procedures. The term linear viscoelastic behavior implies that the principles of proportionality and superposition were both met.

For a short term (less than 10 hours) creep test, the *log* compliance versus *log* test time data for both S_{22} and S_{66} tests will appear as shown in the example provided by figure 1. A three parameter expression modeled the test data.

$$S_{ij}(t) = S_{ij}^{o} e^{(t/\tau)^{\beta}} \tag{2}$$

Where S_{ij} is the time-dependent creep compliance term from equation 1, S_{ij}^{o} is the initial creep compliance, t is time , τ is the characteristic retardation time and β is the shape parameter. The fitting algorithm was based upon the Levenberg-Marquardt method[6]. For the continuous fiber reinforced composite, the individual terms can be written:

$$S_{22}(t) = S_{22}^{o} e^{(t/\tau_2)^{\beta_2}}$$
$$S_{66}(t) = S_{66}^{o} e^{(t/\tau_6)^{\beta_6}} \quad (3)$$

The short term creep compliance curves as shown in figure 1 had a horizontal or time shift between curves defined by *log* a, and the vertical or initial compliance shift between curves defined as *log* b. Figure 1 schematically illustrates these shifts. It was assumed that both shifts were due to physical aging effects.

Once the time shifts (*log* a) were measured for a given set of compliance tests, the aging shift rate (μ) was calculated using

$$\mu = \frac{d\log(a_{te})}{d\log(t_e)} \quad (4)$$

where t_e is the specific aging time for a given test. Struik[1] indicates that for sub-T_g temperatures the shift rates would be constant over the relatively short aging time of a test sequence and would have a value close to unity. By raising the test temperatures sufficiently close to T_g, Struik[1], and Lee and McKenna[7], found the shift rate of an aging test decreased significantly below unity. This was attributed to the material approaching an equilibrium state. The time required to reach this equilibrium state is dependent on the test temperature. Lee and McKenna[7] have stated that this equilibrium time was not dependent upon the state of stress. An empirical formula for estimating this equilibrium time (t_∞) for polymers was given by Struik[1] to be

$$t_\infty \cong 100e^{.77(T_g - T)} \quad (5)$$

where T is the test temperature in degrees C and t_∞ is in seconds.

Test Material and Specimen Configuration

The composite material used in this study was a continuous carbon fiber reinforced amorphous thermoplastic fabricated by AMOCO and designated IM7/8320 (formally IM7/RadelX). Static lamina properties measured isothermally and given previously[8] are repeated for reference purposes in table 1. The T_g as measured by a DSC , was 221.3°C.

The static material property tests were run using a rectangular specimen geometry of approximately 9.5"x1" with a 12 or 8 ply thickness with a set of thin end tabs added to each end of the specimen. For the creep tests, the transverse (S_{22}) and shear (S_{66}) compliance data came from $[90]_{12}$ and $[\pm 45]_{2s}$ specimens respectively.

Test Procedures and Equipment

Before testing, all specimens were dried for at least 15 hours at 110°C in a convection oven. After drying, the specimens were desiccated until the start of the testing. After each test sequence the specimens were inspected for matrix cracks along their edges with an optical microscope.

Three test temperatures selected for study were 195°, 200° and 212°C. The two lower temperatures provided data near the upper use temperature of the material. The highest test temperature was selected to ensure that the aging to a point near equilibrium would occur within a reasonable amount of time. For IM7/8320, which has a T_g of 221.3°C, the aging time to equilibrium based upon equation 5 would vary from 35.2 hours for the upper test temperature of 212°C, to 17.3×10^6 hours for the lower test temperature of 195°C.

All of the creep tests were performed in convection ovens equipped with digital controllers. Temperature monitoring and feedback thermocouples were placed near the test section. Thermal apparent strain was corrected for by using the compensating gage technique[9]. Load was applied through a dead-weight cantilever arm and reacted at a point outside the test chamber. Mechanical wedge grips held the specimen during the loaded or creep segments. Stress was calculated based upon the applied load and the specimen cross section measured before testing. During the unloaded or recovery segments, the lower grip was released using a remote cable and pulley system. This mechanism allowed the test chamber to remain closed during the entire test sequence.

Strain in the gage section was measured with high temperature foil strain gages applied in the center of the specimen. The gage type was Micro-Measurement WK-00-250BG-350 with the Mbond-600 gage adhesive. Proper selection of gage type and adhesive gave CTE match and stability at elevated temperatures.

For the $[90]_{12}$ specimens, the average measurement of two back-to-back gages, aligned longitudinally, were used to compute S_{22}. For the $[\pm 45]_{2S}$ specimens, the average measurement in each direction of four gages, two back-to-back aligned longitudinally and two back-to-back aligned transversely were used to compute S_{66}. The compliance terms for these specimens are as follows:

$$S_{22}(t) = \frac{\varepsilon_x(t)}{\sigma_x}$$

$$S_{66}(t) = \frac{2\varepsilon_x(t)[1-\varepsilon_y(t)/\varepsilon_x(t)]}{\sigma_x} \tag{6}$$

Each gage formed a quarter-bridge circuit. Thermal strain compensation was accomplished during data reduction. Commercially available instrumentation provided bridge completion, excitation and signal conditioning. A personal computer equipped with a 12-bit A/D board converted and stored for later analysis the high level analog output signal from the amplifiers.

Creep Compliance and Physical Aging

A procedure for measuring creep compliance, as described in Struik[1], was used for all tests. This procedure consisted of a sequence of isothermal creep and recovery tests. Each creep period was short in comparison with the previous aging time. During the aging process, the short term creep tests required a constant load. After each creep segment, the specimen was unloaded and allowed to recover until the start of the next creep test. Figure 2 is a schematic of this procedure. Table 2 provides the temperatures and applied axial stress for each test sequence.

As part of the test procedure, immediately before the start of any physical aging test sequence the specimen was held at 235°C (approximately 15° above it's T_g) for 15 minutes and then rapidly quenched with compressed air to the test temperature. This excursion above the T_g rejuvenates the specimen and erases any prior physical aging history. After reaching the test temperature during the quench, the aging time started.

The ratio between the prior aging time and each creep test time was at least 10:1 for the sequenced tests. Using this ratio and the sequencing procedure, up to 7 creep tests were conducted during an aging time of approximately 120 hours. One point of concern for such sequenced tests is the effects of repeated loading on the aging process. To check out such loading effects, sequenced creep tests were run for 27 hours aging (3 loading segments). The 27 hour sequenced compliance data was then compared to data from a specimen with the same 27 hours aging time but without the intermediate creep segments.

During the creep recovery segments of each aging test sequence, the specimen had no load on it. The recovery times were long enough to allow for nearly complete strain recovery. However, to account for any remaining strain, the strain measured in the creep segment was corrected by subtracting the extrapolated prior recovery curve from the creep curve as shown in figure 2. To further investigate the effects of short versus long recovery times, two sets of sequenced creep/recovery tests were run with identical aging times but different creep/recovery times. Figure 3 is a schematic illustrating these two test schedules.

Thermoreversibility of Physical Aging

Due to the supposed thermoreversibility of the physical aging process, a single specimen could be used for several aging tests as long as the rejuvenation occurred before each test sequence. This reversibility was verified by measuring creep compliance from a single specimen loaded several times with a rejuvenation sequence before each loading.

Determination of Applied Stresses

For linear viscoelastic behavior, it was assumed that superposition and proportionality would hold. Given an initial state of stress σ' applied for a time t and an additional stress σ'' applied at a time t_1, superposition implies that:

$$\varepsilon[\sigma'(t)+\sigma''(t-t_1)]=\varepsilon[\sigma'(t)]+\varepsilon[\sigma''(t-t_1)] \qquad (7)$$

while proportionality states that for an applied stress σ, the strain in a material at any other stress state is found using:

$$\varepsilon[c\sigma(t)]=c\varepsilon[\sigma(t)] \quad \text{where} \quad c=\text{constant} \qquad (8)$$

Creep and creep/recovery data from several loadings at different stress levels provided data for checking superposition. Proportionality was checked by plotting isothermal, isochronous stiffness versus applied stress for a specimen that was repeatedly rejuvenated, quenched and loaded at increasingly higher stress levels. The supposed transition from linear to nonlinear behavior should be evident by a slope change in the data.

Results: Tensile Creep Compliance

Results from the experiments illustrate the effects of stress and physical aging on the elevated temperature creep compliance of IM7/8320. Superposition, proportionality, sequencing effects, load duration effects, stress overload effects, aging to equilibrium, aging shift factors and aging shift rates were measured and quantified.

Superposition

For linear viscoelastic behavior, superposition should hold. For the creep test, superposition states that the recovery strain can be found using equations 2 and 7 such that:

$$\varepsilon(t^*) = \sigma S^o \left\{ e^{(t/\tau)^\beta} - e^{\left((t-t_1)/\tau\right)^\beta} \right\} \tag{9}$$

Where σ is the constant stress, t_1 is the time of load removal, t^* is the time during the recovery segment and S^o,τ and β are the constants from the measured creep compliance curve. Equation 9 was used to predict the recovery of a $[90]_{12}$ transverse specimen loaded at sequentially higher load levels. The specimen was rejuvenated before each test and aged for exactly 30 minutes before loading. Figure 4 provides the predicted strain/time curves along with the measured data.

Comparison of test and prediction for the recovery segments indicates that only the recovery test data at the lowest load level was accurately predicted by superposition. However, the predicted strain rate during recovery corresponded well with the measured value for all load levels tested.

Proportionality

One of the clearest ways to check if proportionality holds for creep tests is to plot the isochronous stiffness versus applied stress levels at a constant temperature. The stiffness values were calculated by inverting the measured creep compliance data for any given time during the loaded segment of the test. Unproportional behavior will be evident by deviations from linearity of the data as stress increases. Figures' 5-8 give examples of such data.

Figures 5 and 6 indicate little or no unproportional behavior as a function of applied stress whereas figure 7 and 8 show a transition to unproportional behavior. Comparing figures 5-7 shows that these deviations from linearity became more apparent as the test temperature increased. The stress levels chosen for the aging experiments are indicated upon these figures. Using the isochronous stiffness data from figures' 5-8, the aging test stress levels were chosen to correspond to the range where little or no deviation from proportionality was observed.

Sequencing Effects

To ensure that the sequencing procedures of the momentary creep tests worked, checks were made using different specimens and test temperatures. For the sequencing to work properly, any creep compliance data from the sequenced creep/aging experiment should coincide with an unsequenced creep compliance measurement taken at the same aging time. Figure 9 shows an example of this behavior for a $[\pm 45]_{2S}$ specimen loaded at 1,3, 9 and 27 hours of aging time versus the same specimen loaded only at 27 hours aging. Both tests included a rejuvenation period before the start of aging.

Examination of the compliance data in figure 9 indicates that the sequenced tests produced equivalent 27 hour compliance data compared to the unsequenced test. This demonstrates that the short loading periods of the sequenced tests did not measurably effect the data, thereby ensuring that the sequenced test procedure gave a true measure of physical aging.

Load Duration Effects

The momentary creep compliance measured during the aging tests was essentially a "snapshot" of the aging process. This required that the duration of a creep segment be kept much lower than the cumulative aging time, thereby ensuring minimal influence on the aging process moreover allowing for a sufficient time for strain recovery to occur. The data from all the strain recovery segments of the sequenced creep compliance measurements indicated that near complete recovery took place. As suggested by Struik [1], the unrecovered strain was subtracted from the total strain during the following creep segment. The unrecovered strain was computed using a linear extrapolation of the steady state portion of the creep recovery curve. Figure 2 schematically illustrates this procedure.

To explore the effects of load duration on creep compliance, two different test schedules were followed. Figure 3 gives the times for the creep and recovery segments of these two test schedules. The test sequence with the short creep segments was designated Schedule 1 and the test sequence with the long creep segments was designated Schedule 2. Figure 10 shows the measured effects on creep compliance due to loading according to these schedules.

Figure 10 clearly illustrates that the extended creep times used in Schedule 2 produce different creep compliance curves than the data from Schedule 1. The differences are due to the additional creep occurring during the extended load time. If the curves from both schedules are fit with equation 2, different parameters will result. However, the effects of aging (*log* a shifts) are apparent using either test schedule. For material systems unlike IM7/8320 that would not exhibit such rapid strain recovery, the effects of extended load periods would become even more pronounced.

Stress Overload Effects

As outlined by Struik [1], a momentary stress overload during a normal sequenced creep compliance test for aging may upset the aging process in the material. He states that if this overload is sufficiently high, the material may apparently deage. To explore this idea, a sequenced creep compliance test was run on a $[90]_{12}$ transverse specimen at 200°C. Figure 11 shows the load/time history imposed on this specimen. For the first three segments of the sequenced test, the load was kept at a constant. The aging time for these segments was 1, 3 and 9 hours. The forth segment occurred at 24 hours and consisted of an overload that was approximately 1.7 times the previous load. The initial load was then used for the subsequent segments. To capture any immediate or transient effects on the aging process,

the segments after the overload started at 1,3,9 and 26 hours after the overload was removed or 26,28,34 and 51 hours total aging time respectively.

Figure 12a gives the resulting creep compliance curves. The 1,3,9 and 24 hour aging time segments collapsed to form one momentary master curve referenced to the 1 hour curve. The 26,28,34 and 51 hour aging time segments collapsed to form a momentary master curve referenced to the 26 hour curve. Apparently these curves are distinct in both shape and location.

Figure 12b gives the resulting shift factors. All the factors are first plotted using the 1 hour curve as a reference for all the data. As shown in the figure, a slight disruption of the data occurs after the overload. However, deviations from linearity of the shift rate (μ) are not significant. Fitting all the data gave a shift rate of .90. If just the post-overload shift factors are plotted referenced to the 26 hour test, the shift rate decreased to .30.

Aging to Equilibrium

An experimental study on the ability to age the material to a state near equilibrium was performed using S_{22} specimens tested at 212°C and four stress levels. Figures 13 and 14 give the shift factors for these tests. Shift factors used in figure 13 are from using only the horizontal time shift to create the master curves. Figure 14 shows results from the same tests but with the time shifts computed after a vertical compliance shift. A bilinear least squares fit to the data was computed for all four data sets and is shown in figures 13 and 14. The break in these bilinear fits was made at the 3 hour aging point. Additional data points before and after this 3 hour point would further define these break points. The 3 hour data point for the 385psi data set was not included in the curve fit due to excessive scatter.

A comparison of figures 13 and 14 show that inclusion of the vertical shift in the collapse of the data to form the master curve may decrease the scatter of the aging factors. However, the general trends in the data do not change by including this vertical shift.

Aging Shift Factors

Given a set of momentary creep compliance curves as shown in figure 1, the time shift factors (*log* a) for each curve were measured by referencing all curves to the first (1 hour) creep compliance curve. To facilitate computation of these shift factors, each curve was fit with the three parameter model shown in equation 2. The smooth curves generated from these fits were shifted along the time axis until they coincided with the reference curve and therefore created a momentary master curve. The master curve data was also fit with equation 2. Table 2 gives the three parameters from the analysis of the master curve data for the 195° and 200°C sequenced tests. Figures' 15-18 provide the master curves for S_{22} and S_{66}.

For many of the tests a vertical or compliance shift would facilitate the collapse of the data. However, the time shifts due to aging were of primary importance in this study, therefor all the shift factor and shift rate curves shown in the results were found using the time (*log* a) shifts only unless otherwise noted.

Figures' 19-22 present the time shifts versus aging time. In these figures, a linear least squares fit to each data set is also shown. Each linear fit represents a different applied stress level. Figures 19 and 20 are the S_{22} data at 195°C and 200°C respectively. Figures 21 and 22 are the S_{66} data at 195°C and 200°C respectively. All the data presented in these figures have a data point at the origin.

Aging Shift Rates

The aging shift rates for all tests were computed by using linear least squares fits to the aging shift factors. Tables 2 and 3 give the computed shift rates. Figure 23 is a plot of these shift rates as a function of applied axial stress. The S_{66} data at 195°C and 200°C collapsed and was fit with one curve. The S_{22} data sets for each temperature were separate and fit with their own curves. The shift rates shown in figure 23 for the S_{22} specimen at 212°C are values from the secondary slope of the bilinear fit. These rates were computed using shift factors found from the aging time shift to the data.

Figure 24 uses the same shift rate data as in figure 23 but shows it as a function of ply stress for the S_{22} and S_{66} specimens. The transverse stress (σ_{22}) in the 90° ply of the S_{22} specimen is equal to the applied axial stress. The shear stress (σ_{12}) in a 45° ply of the S_{66} specimen has a magnitude equal to one half of the applied axial stress. The 195°C, S_{66} specimen tested at 960psi was the only specimen in which damage (transverse matrix cracks) was detected during post test inspection. This data point was not used in the curve fit of figure 23 or 24.

Discussion and Summary: Tensile Creep Compliance

Linear viscoelasticity assumes that both proportionality and superposition hold. Data from figures' 4-8 reveals the difficulty in checking these concepts for elevated temperature PMC's. The inability of superposition to accurately predict strain recovery for all stress levels indicates some stress level dependency. However, the proportionality data suggests that there should be a range of stress levels available for testing in the linear viscoelastic range. For temperatures sufficiently close to the T_g, PMC's may exhibit non-linear behavior in the matrix constituent. The lack of a sharp transition from linear to non-linear behavior would suggest that if test stress levels are low, linear viscoelasticity may provide a first level approximation when developing test and analysis procedures.

The sequenced creep/recovery procedures seem to work well for characterizing physical aging in PMC's. It appears necessary to keep the ratio between aging time and test time to a value of 10 or greater to ensure that loading has a minimum influence on aging and that the material has sufficient time to undergo strain recovery.

The tests on the S_{22} specimen at 212°C indicated that if the temperature was sufficiently close to the T_g, a change in the aging shift rate may occur. Figures 9 and 10 indicate that these breaks in shift rate, or time to equilibrium, are relatively independent of applied stress level. This result has important implications for long term testing. The aging towards equilibrium behavior for the IM7/8320 material was similar to the results achieved by Lee and McKenna[7] for epoxy glasses.

Momentary master curves do not reveal a clear trend when examined as a function of stress level. Examining figures 15-18 show that in general the master curves will shift to the right along the time axis as stress level increases. However, the data does not appear to lend itself well to a time-stress superposition type of analysis. The plots of shift factor versus aging time given in figures' 19-22 verify the trend in shift factors as a function of applied stress.

Plotting shift rate (μ) as a function of applied axial stress, as in figure 23, indicates that μ for the two creep compliance terms have different aging shift rates. The S_{22} term shows a higher dependency

on applied axial stress. In addition, the S_{22} data shows some temperature dependency when compared to the S_{66} data. This difference in temperature dependency between the two compliance terms is probably due to the low creep strains of the S_{22} data and the inability of the instrumentation to accurately resolve strains less than 10με. The S_{66} data gave less scatter at both test temperatures.

Struik[1] has shown that the shift rate (μ) of rigid PVC loaded under two separate loads, tensile and shear, will collapse when plotted against applied stress. This stress was assumed to be large and to cause non-linear creep. He further states that the collapse of the μ/stress data appears to be independent of test temperature. Plotting the shift rates from table 2 as a function of ply stress, as in figure 24, indicated the data for the S_{22} and S_{66} specimens may collapse into a single data set where the temperature and load type dependency are less apparent.

Struik[1] has interpreted this stress level dependency in polymers as an indication that large stresses produce an erasure or deaging of the material. Lee and McKenna[7] have offered an alternative interpretation of the decrease in shift rate as a function of an increase in the applied stress. They state that "an increase in the amplitude of the stress applied in the physical aging experiment results in a decrease in the shift rate μ simply because the changes in structure accompanying volume recovery affect the non-linear response differently at large stresses than at small ones." They further state that this does not imply that the structure of the polymer is changed by the application of mechanical loads. At this point, the authors feel that additional data on the composite material is needed to fully validate either of the theories presented.

TENSILE ELASTIC/VISCOPLASTIC BEHAVIOR

In previous reports by the author [8], [10], a elastic/viscoplastic analysis model was developed to predict the nonlinear, rate and time-dependent behavior of PMC's at stress levels approaching tensile ultimate. The model was verified by comparison to test data from matrix dominated laminates at elevated temperatures. These tests were short term (on the order of minutes) and the effects of extended exposures at temperature were not studied. However, as the need for accelerated test methods grows, the time scale of the characterization tests must also increase.

Significantly fewer studies have been conducted on the effects of physical aging on the nonlinear behavior of PMC's. In a study of an epoxy resin, Augl [11] used a nonlinear viscoelastic formulation to look at the effects of physical aging on the creep response. More recently, Lee and McKenna [7] performed creep compliance tests to develop the relationships between physical aging and stress in polymers.

The lack of work in characterizing such behavior in PMC's has motivated the current research and provided the objective that was to assess the effects of physical aging on the nonlinear stress/strain behavior of a typical high temperature PMC. The elastic/viscoplastic constitutive model developed previously provided the means for quantifying this aging effect.

Constitutive Model

The elastic/viscoplastic constitutive model predicted many of the experimentally observed short term phenomena in matrix dominated laminates over a range of typical operating temperatures. The model is macromechanical and phenomenological in form. An undamaged state was assumed for the laminate.

Assuming plane stress conditions for in-plane tension loading, the total strain rate was assumed to be composed of elastic and viscoplastic components as follows

$$\begin{aligned}\{\dot{\varepsilon}\} &= \{\dot{\varepsilon}^{e}\} + \{\dot{\varepsilon}^{vp}\} \\ &= [S]^{e}\{\dot{\sigma}\} + [S]^{vp}\{\dot{\sigma}\}\end{aligned} \tag{10}$$

The elastic compliance term was assumed to be linear and independent of stress level. In general, it was a function of the elastic moduli such that

$$[S]^{e} = \begin{bmatrix} 1/E_1 & -\nu_{12}/E_1 & 0 \\ -\nu_{12}/E_1 & 1/E_2 & \\ 0 & 0 & 1/G_{12} \end{bmatrix} \quad \textit{elastic compliance.} \tag{11}$$

The terms E_1, E_2, G_{12}, and ν_{12} are elastic constants referenced to the material principal axis. On the basis of the viscoelastic behavior of IM7/8320 as observed by Hastie and Morris [3], it was assumed that only the transverse (E_2) and the shear (G_{12}) moduli were functions of aging time.

The viscoplastic compliance was found to be a nonlinear function of stress and was partially derived using the overstress concept as follows

$$[S]^{vp} = [S]^{vp'} + [S]^{vp''} \quad \textit{viscoplastic compliance} \tag{12}$$

The first part of the viscoplastic compliance matrix was found to be

$$[S]^{vp'} = \gamma \frac{3}{2\bar{\sigma}} \left(\frac{\langle H \rangle}{K} \right)^{1/m} \begin{bmatrix} 0 & 0 & 0 \\ 0 & \left(\sigma_{22}/\dot{\sigma}_{22}\right) & 0 \\ 0 & 0 & \left(2a_{66}\sigma_{12}/\dot{\sigma}_{12}\right) \end{bmatrix} \tag{13}$$

and the second term in equation 9 was found to be

$$[S]^{vp} = \frac{\dot{\bar{\sigma}}(n-3)}{3\bar{\sigma}}\Psi\begin{bmatrix} 0 & 0 & 0 \\ 0 & \left(\sigma_{22}^3/\dot{\sigma}_{22}\right) & 0 \\ 0 & 0 & \left(4a_{66}^2\sigma_{12}^3/\dot{\sigma}_{12}\right) \end{bmatrix} + [S]^{qp} \tag{14}$$

In equations 10 and 11, the terms n, K and a_{66} are material constants and the terms σ_{22} and σ_{12} are the inplane transverse and shear stress components, respectively.

Overstress, defined as the difference between the rate-dependent (σ) and rate-independent (σ^*) stresses was given as

$$H = \left(\bar{\sigma} - \bar{\sigma}^*\right) \tag{15}$$

where the bar indicates the effective stress.

The theoretical lower bound of the rate dependent behavior was represented by a rate-independent (quasistatic) elastic/plastic constitutive relation developed by Sun and Chen [12] where

$$\{d\varepsilon^{qp}\} = [S]^{qp}\{d\sigma^*\} \tag{16}$$

For functional relationships that relate the plastic and viscoplastic material constants to measurable test data,

$$H = K\Phi^m \tag{17}$$

$$\bar{\varepsilon}^p = A\bar{\sigma}^n \tag{18}$$

where Φ is the effective plastic strain rate and ε^p is the plastic strain. Analysis of a laminated plate required incorporating the constitutive equations into a form of lamination theory that was solved numerically by updating the compliance matrices using the previous stress state. For an orthotropic plate, the constitutive equations reduced to a first order nonlinear differential equation that was solved using a numerical integration technique.

Test Procedures and Equipment

The general testing procedures developed in [13] for unaged materials were used to develop the material constants for the aged specimens. Key points and differences due to the inclusion of aging effects are noted in the following paragraphs.

For the elastic/plastic and elastic/viscoplastic material constants, multiple off-axis tests were run on $[25]_{12}$, $[30]_{12}$, and $[40]_{12}$ specimens. These angles produced a high degree of plasticity before failure.

Data from these off-axis tests were then used to construct material master curves. All tests were conducted under isothermal conditions using strain controlled, tension loading. Microscopic examinations of the specimen's edges after each test checked for damage induced by testing.

Heat from an internally heated aluminum test fixture was directly transferred to the test specimen along the entire ungripped length and across the entire width of the specimen. This fixture was used for both aging and testing the specimens. The test temperature selected for this study was 170°C.

Extensometers measured the axial strain. The load frame was a servo hydraulic test machine capable of running predetermined strain-history profiles. Load, as measured by the load cell, was converted to stress using the average cross-sectional area of the specimen measured before testing.

Before the start of any physical aging test sequence the specimen was held at 235°C (approximately 15° above it's T_g) for 10 minutes and then rapidly quenched with compressed air to the test temperature. This excursion above the T_g rejuvenates the specimen and erases any prior physical aging history. Aging time in this study refers to the time at temperature following the quench and before the start of the test. Aging times selected for this study were .5, 25, and 65 hours. All the material property tests were run with the same test time (under load) history, therefore, any aging during the test was discounted. However, any extensions of this work to long term cyclic tests would require the inclusion of the test time into the total aging time.

Uniaxial strain controlled tests of off-axis specimens [13] generated the inelastic material constants. These tests required repeated holds to allow for stress relaxation. For the tests performed in this paper, these holds were 20 minutes each. The length of the hold time was approximately the same as the time scale of interest for the modeling. The minimum stress reached during such a relaxation segment is the quasistatic stress and defines the rate-independent response. Besides quantifying these quasistatic stress levels, the relaxation segments provided stress versus time data that was used to define the rate-dependent response.

Results: Tensile Elastic/Viscoplastic Behavior

The formulation of the constitutive equations required that the material properties be found from uniaxial tests of off-axis specimens. Therefore, many of the results presented herein will deal with the response of off-axis tests.

Thermoreversibility of Yield

Figure 25 shows the axial stress/strain behavior of an off-axis specimen. Each of the four tests was run on the same specimen immediately after a rejuvenation and quench to the test temperature. On the basis of the repeatability of the curves, it appeared that yielding of an off-axis specimen is a thermoreversible process. Struik [1] shows that this type of reversible process also occurs for neat resins.

Ductility

Variations in aging temperature effected the aging process and therefore the measured stress/strain response. Figure 26 illustrates typical measured behavior by comparing experimental stress/strain data from two off-axis orientations. As shown in figure 26 and in the accompanying table, given two specimens that are identical except for aging temperature, a higher aging temperature will result in a higher failure strain. Since a higher aging temperature will increase the aging rate, the measured trend is towards increased brittleness as aging progresses. Similar results were also found by Struik [1] and Chen et.al. [4].

Plasticity

Figure 27 shows the effects of aging time on the quasistatic elastic/plastic stress strain behavior of two off-axis orientations. These curves were fit to the minimum relaxation points of a test. The small insert figure shows the accuracy of the fit to the relaxation points for a representative test. The quasistatic curve represents rate-independent elastic/plastic behavior and is clearly a function of aging time. An increase in stiffness occurred due to an increase in aging time. Figure 27 also illustrates the relative sensitivity of the different off-axis angles to the aging process. It appears that the more highly coupled $[25]_{12}$ specimen was more sensitive to aging time. For comparison, figure 27 gives the quasistatic curve from an unaged, as-received specimen.

Using procedures similar to those described in [13], effective stress/effective plastic strain data was measured for three aging times. Figure 26 gives this data and the best fit to this data. These curves were material master curves. As expected from the quasistatic data of figure 27, the plasticity master curves of figure 28 are also a function of aging time. These master curves were fit with equation 18 using a constant exponent (n=4.66) and allowing the parameter A to vary with aging time. Figure 29 shows this variation of A. Table 4 lists this data. For comparison purposes, the variation of A with test temperature from reference [10] is given in figure 25 for unaged, as-received specimens. Comparing figures 29 and 30 shows that the change in A due to aging 65 hours is on the same order of magnitude as a change in test temperature from 150°C to 175°C. The material constant a_{66}=.3, determined through the process of collapsing the master curve data, was insensitive to aging time.

Viscoplasticity

The constants K and m of equation 17 are the constants of interest for characterizing the effects of physical aging on the rate-dependent elastic/viscoplastic behavior. Using procedures similar to those described in [13], the overstress/effective plastic strain rate data was collected for three aging times. Figure 31 gives this data along with the master curves (fit using equation 17). Table 4 gives numerical values. For these three master curves, the exponent (m=1.) was fixed and the constant K was allowed to vary with aging time. Figure 32 shows this variation of K with aging time. For comparison, figure 33 gives the variation in K with test temperature for unaged, as-received specimens. The change in K for both figures 32 and 33 was less than one order of magnitude over the range of aging times and temperatures investigated.

Model Verification

Once the constants required for the constitutive model were determined from tests, comparisons were made between test data and analytical predictions. Figure 34 shows typical stress/strain curves for comparison between test and prediction of off-axis specimens. Both sets of test data in figure 34 had multiple relaxation events occurring over the course of the test. The minimum relaxation point was representative of the rate-independent (plastic) behavior. The $[25]_{12}$ off-axis specimen in figure 34 was aged for 7 hours before starting the test. This represents an aging time that was not investigated directly when determining the material constants in table 4. Material constants used for prediction of this 7 hour test response were interpolated from the known data at .5 and 25 hours aging. The $[60]_{12}$ off-axis specimen, aged for 65 hours, was not used in construction of the master curves of figures 28 or 31. Therefore, the predicted behavior of the $[60]_{12}$ specimen represented a true prediction and not a verification of data used as input to the model. Both sets of data in figure 34 indicate that the model did a good job of predicting both the viscoplastic and plastic response of off-axis specimens.

The constitutive model required the lamina elastic constants given in equation 11 as partial input. The 170°C constants for unaged IM7/8320 were determined by interpolating between the known data at 150°C and 175°C given in reference [10]. Reductions in E_2 and G_{12} due to aging were found by using the changes in initial elastic properties of IM7/8320 given by Hastie and Morris [3] at 170°C. The resulting constants are given in table 4 for reference. Elastic constants unaffected by aging were E_1=153.9(MPa) and ν_{12}=.32.

Additional verification of the constitutive model was made by comparison of test and prediction for matrix dominated angle-ply laminates tested under constant strain rate conditions. Figure 35 shows two sets of stress/strain data and their associated predicted behavior. Table 4 provided the material constants used in the analytical prediction. The comparison between test and prediction indicated that the model can satisfactorily predict the laminate response over the initial strain levels with an increasing level of error as the strains increase. These specimens were not tested to failure. A maximum strain level of .004 was selected for comparison to the model based upon the range of strains used to find the material constants (e.g., figure 27).

Prior work with unaged, as-received specimens [8] verified the accuracy of the model to account for nonlinear, rate-dependent behavior in undamaged angle-ply laminates. All the aged, angle-ply laminates investigated is this study revealed some degree of matrix cracks during post-test examination. These cracks would either be transverse ply cracks, longitudinal delaminations, or some combination thereof. The two specimens tested for figure 35 revealed only longitudinal delaminations during inspection. As shown by O'Brien [14], this type of damage will not decrease the longitudinal elastic stiffness of the laminate. However, the effects of the delaminations on inelastic stress/strain behavior have not been investigated.

After all the material constants were found at specific aging times, the constitutive model was used to analytically explore the effects of physical aging on various aspects of nonlinear, rate-dependent behavior. For example, Figure 36 gives predicted stress/strain curves for two classes of angle-ply laminates as a function of aging time. Both the plastic and viscoplastic curves are shown. An increase of inelastic stiffness due to an increase in aging time is evident in figure 36. The predictions showed that

the changes in elastic response due to aging became insignificant when compared to the effects of aging in the inelastic, rate-dependent regimes.

Figure 37 shows the predicted effects of aging time on short term creep (20 minutes) of an off-axis specimen loaded well beyond the linear viscoelastic level. The small insert figure shows the corresponding predicted stress/strain curves for the predicted creep curves. These curves illustrate the dependency of creep on the prior aging time. As shown, for two creep tests started at the same initial strain, the higher initial stress due to increased aging time will result in a larger creep strain.

Analogous to the creep curves of figure 37, figure 38 shows aging time effects on stress relaxation curves for off-axis specimens. The normalized stress during relaxation is given versus test time. Both tests were run to the same strain level however aging caused the 65 hour test to have a higher initial stress level. Analytical predictions and test data are given for comparison. Although test and prediction show some differences in magnitude over the 20 minute relaxation time, the test data does verify the predicted trends in initial stress rates and the predicted convergence of the curves as the relaxation time approaches 20 minutes. Oscillations in the test data were due to a low frequency drift of the test machine's strain controller.

Discussion and Summary: Tensile Elastic/Viscoplastic Behavior

Experimental and analytical evidence was presented which showed that physical aging has an effect upon the nonlinear behavior of IM7/8320 at elevated temperature. An increased brittleness due to aging was found to occur in the off-axis laminates used to develop the material constants. Data was also presented that showed the changes due to aging in the elastic response became insignificant when compared to the changes in the inelastic, rate-dependent response.

Four material constants (E_2, G_{12}, A, K) for the elastic/viscoplastic constitutive model were assumed to be sensitive to aging times. Verification of the analytical model indicated that the effects of prior aging on the nonlinear stress/strain/time data of matrix dominated laminates can be predicted. Based upon the measured changes in the stress/strain curves due to aging and the trends in A and K over 65 hours aging time, it was shown that both A and K decreased with increased aging time. The analytical predictions and test data indicated that the changes in stress/strain/time response due to increased aging may be primarily due to the change in the nonlinear rate-independent behavior associated with the constant A.

Acknowledgment

The authors would like to acknowledge the expert technical laboratory assistance of Ms. Lois White and Mr. Reggie Rose.

References

[1] Struik, L.C.E., *Physical Aging in Amorphous Polymers and Other Materials,* Elsevier Scientific Publishing Company, New York, 1978.

[2] Sullivan, J.L., "Creep and Physical Aging of Composites," *Composites Science and Technology,* Vol. 39, 1990, pp. 207-232.

[3] Hastie, R.L. and Morris, D.H., "The Effect of Physical Aging on the Creep Response of a Thermoplastic Composite.", ASTM STP #1174, *High Temperature and Environmental Effects in Polymer Matrix Composites*, Editors, C. Harris and T. Gates, 1992.

[4] Chen-Chi, M., Lee, C., Chang, M., and Tai, N., "Effect of Physical Aging on the Toughness of Carbon Fiber-Reinforced Poly(ether ether ketone) and Poly (phenylene sulfide) Composites. I," *Polymer Composites*, Vol. 13, No. 6, December 1992, pp. 441-447.

[5] Aklonis, J.J., MacKnight, W.J., and Mitchel, S., *Introduction to Polymer Viscoelasticity,* Wiley-Interscience, New York, 1972.

[6] Press, W.H., et.al., *Numerical Recipes, The Art of Scientific Computing,* Cambridge University Press, Cambridge CB2 1RP, U.K., 1986.

[7] Lee, A. and McKenna, G.B., "The Physical Ageing Response of an Epoxy Glass Subjected to Large Stresses," *Polymer*, Vol. 31, March, 1990.

[8] Gates, T.S., "Matrix Dominated Stress/Strain Behavior in Polymeric Composites: Effects of Hold Time, Nonlinearity and Rate Dependency," NASA TM 107595, April 1992, to appear in ASTM STP.

[9] Murry, W.M., and Miller, W.R., *The Bonded Electrical Resistance Strain Gage,* Oxford University Press, New York, 1992.

[10] Gates, T.S., "Effects of Elevated Temperature on the Viscoplastic Modeling of Graphite/Polymeric Composites," *High Temperature and Environmental Effects in Polymer Matrix Composites*, ASTM STP 1174, C. Harris and T. Gates, Ed., American Society for Testing and Materials, 1993.

[11] Augl, J.M., "Nonlinear Creep Effects of Physical Aging, Temperature and Moisture of an Epoxy Resin," *Journal of Rheology*, Vol. 31, No. 1, 1987, pp. 1-36.

[12] Sun, C.T., and Chen, J.L., "A Simple Flow Rule for Characterizing Nonlinear Behavior of Fiber Composites," *Journal of Composite Materials*, Vol. 23, pp. 1009-1020, October 1989.

[13] Gates, T.S., "Experimental Characterization of Nonlinear, Rate-dependent Behavior in Advanced Polymer Matrix Composites," *Experimental Mechanics*, Vol. 32, No. 1, March 1992, pp. 68-73.

[14] O'Brien, T.K., "Characterization of Delamination Onset and Growth in a Composite Laminate," *Damage in Composite Materials*, ASTM STP 775, K.L. Reifsnider, Ed., American Society for Testing and Materials, 1982, pp. 140-167.

Temp. (°C)	E_1 (MPa)	E_2 (MPa)	G_{12}(MPa)	ν_{12}
150	152.9	7.3	4.4	0.33
175	153.9	7.2	3.4	0.32
200	147.0	5.5	2.6	0.35

Table 1. Elastic material constants for unaged IM7/8320 [8].

			Master Curve			
Test Type	Temp(°C)	σ_x (psi)	S^o(1/Gsi)	τ (sec)	β	μ
S_{22}	195	441	880	163970	0.317	1.059
S_{22}	195	539	871	71700	0.356	0.926
S_{22}	195	637	877	102184	0.370	0.856
S_{22}	195	736	888	289175	0.364	0.566
S_{22}	200	337	949	19628	0.357	1.062
S_{22}	200	433	920	29712	0.375	0.894
S_{22}	200	529	914	35919	0.351	0.776
S_{66}	195	665	1644	12733	0.429	1.043
S_{66}	195	813	1633	6224	0.549	0.965
S_{66}	200	506	1683	33758	0.228	1.130
S_{66}	200	650	1850	7074	0.459	1.037
S_{66}	200	794	1768	12283	0.404	0.974

Table 2. Applied Axial Stress, Master Curve Parameters and Shift Rates for the Transverse and Shear Tests. The S_{22} and S_{66} data are from the $[90]_{12}$ and $[\pm 45]_{2s}$ specimens respectively.

S_{22} @212° C

σ_x (psi)	μ^*	μ
200	.132	.239
256	.114	.147
350	.091	.147
385	.065	.147

$\mu^* \Rightarrow$ horizontal shift rate using horizontal and vertical shift

$\mu \Rightarrow$ horizontal shift rate using horizontal shift only

Table 3. Aging Shift Rates for the Secondary Slope of Equilibrium Aging Tests.

Aging time (hrs.)	A (1/MPa)^n	K	E_2 (MPa)	G_{12}(MPa)
0.5	7.16E-09	1710000	7.22	3.66
25	2.03E-09	890000	7.00	3.55
65	1.35E-09	620250	6.93	3.51

Table 4. Material constants for IM7/8320 at various aging times, temperature=170^{o}C.

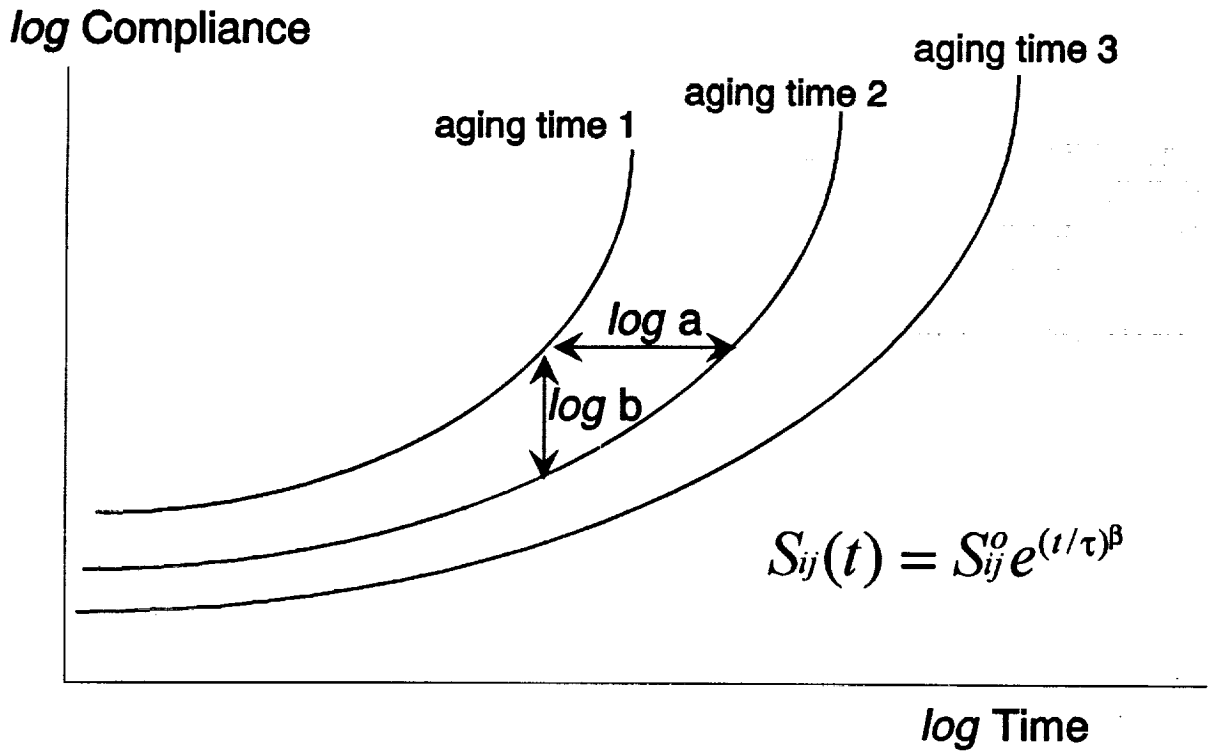

Figure 1. Schematic of typical creep compliance data from a sequenced aging test.

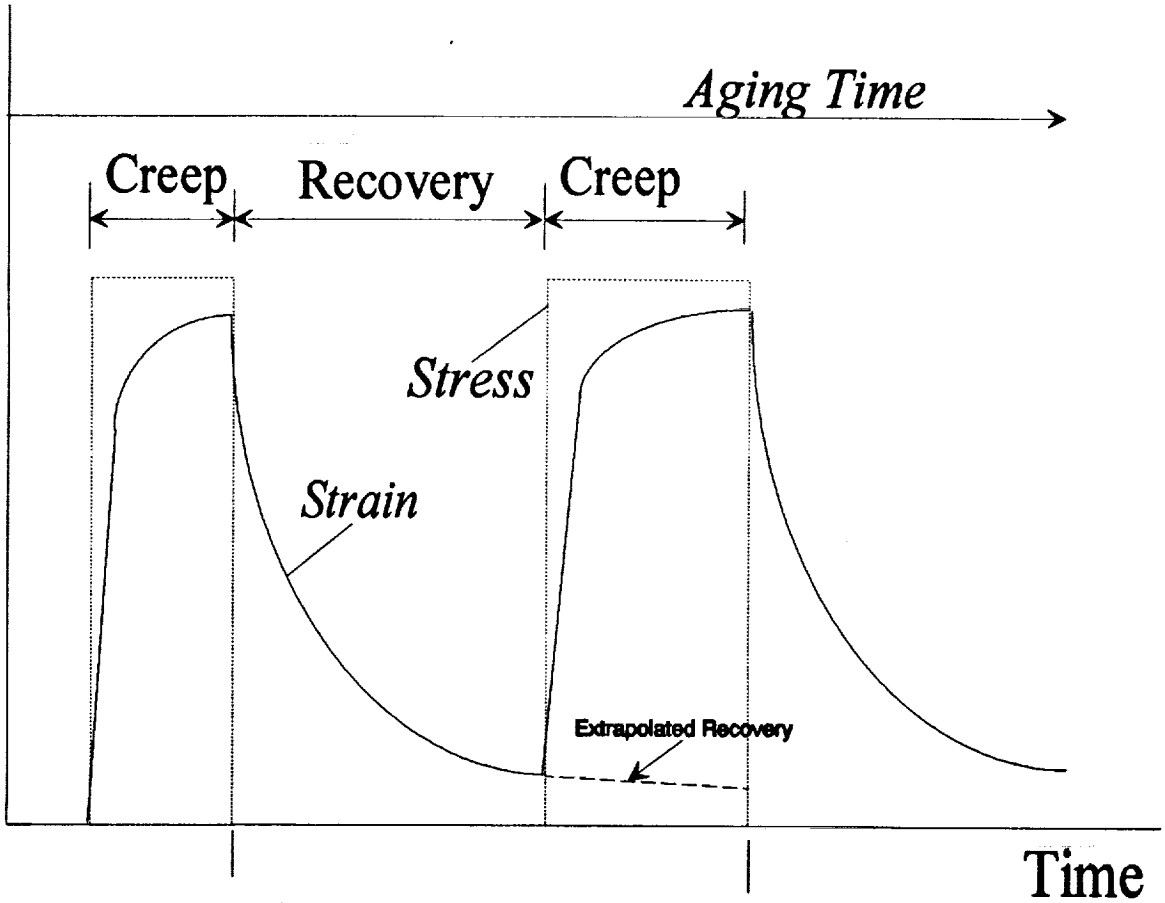

Figure 2. Schematic of creep/recovery sequence for an aging test.

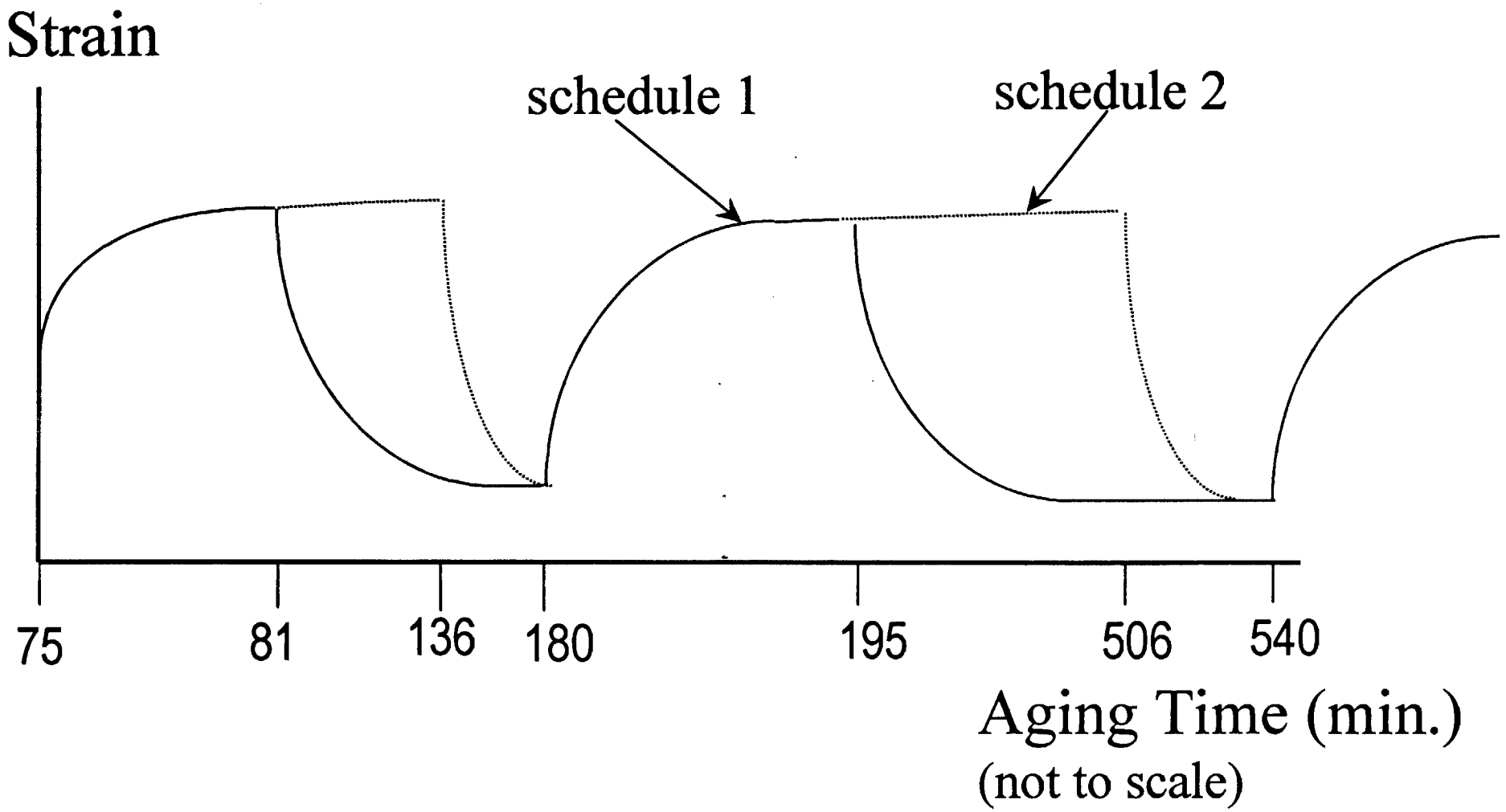

Figure 3. Schematic of creep/recovedry schedules used in tests to asses the effects of load duration.

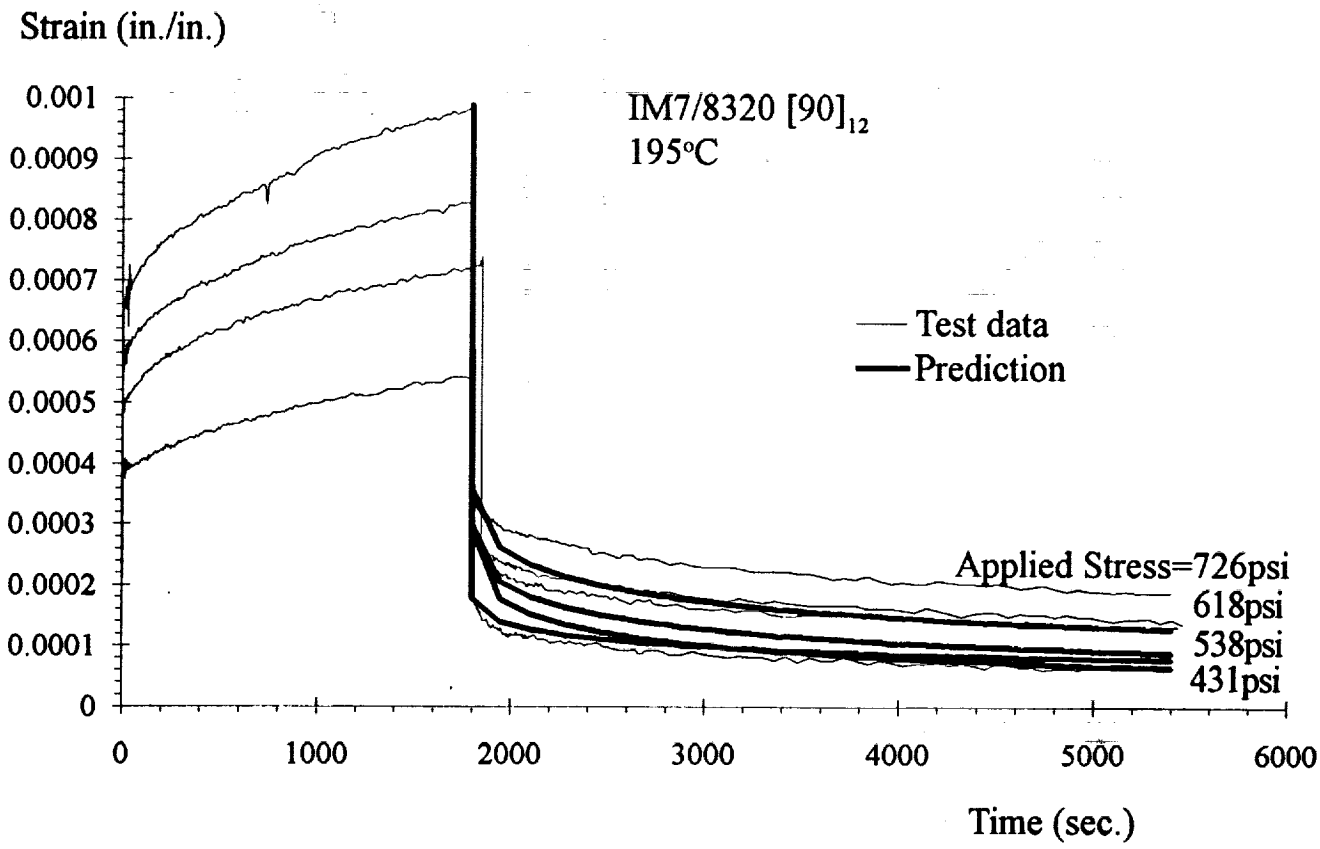

Figure 4. Recovery data versus prediction made using superposition principle.

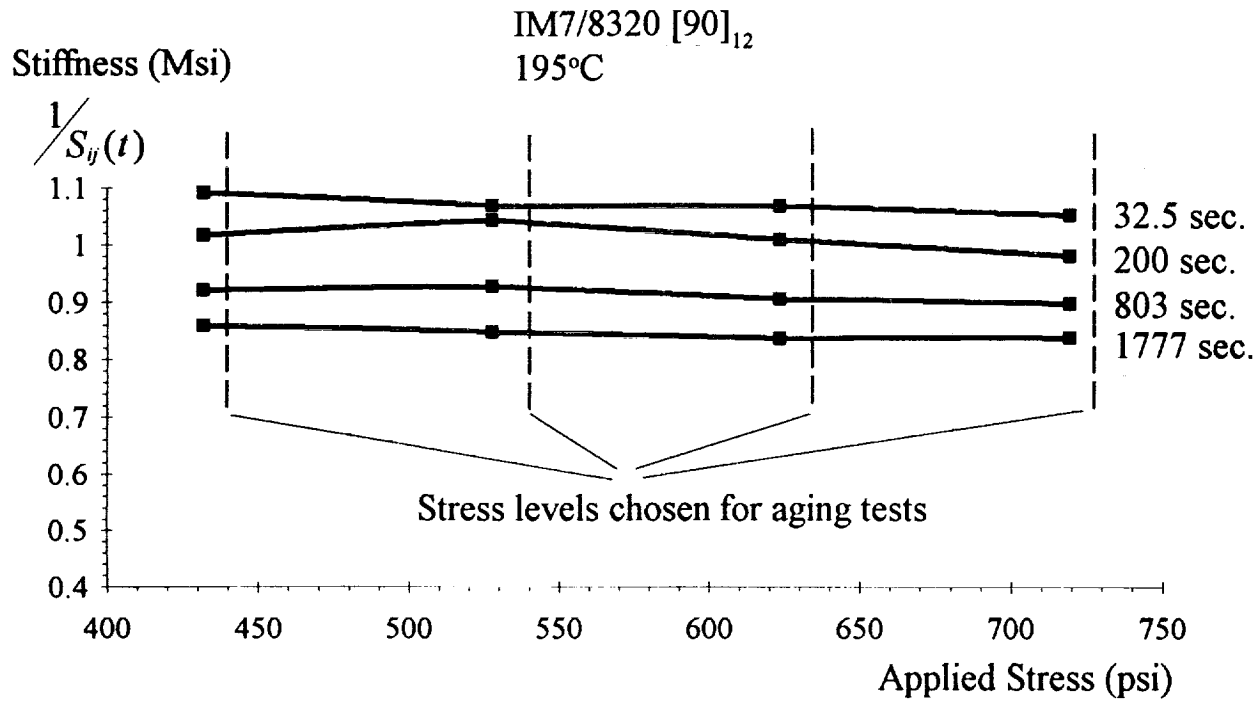

Figure 5. Proportionality check using creep data of transverse specimens tested at 195°C.

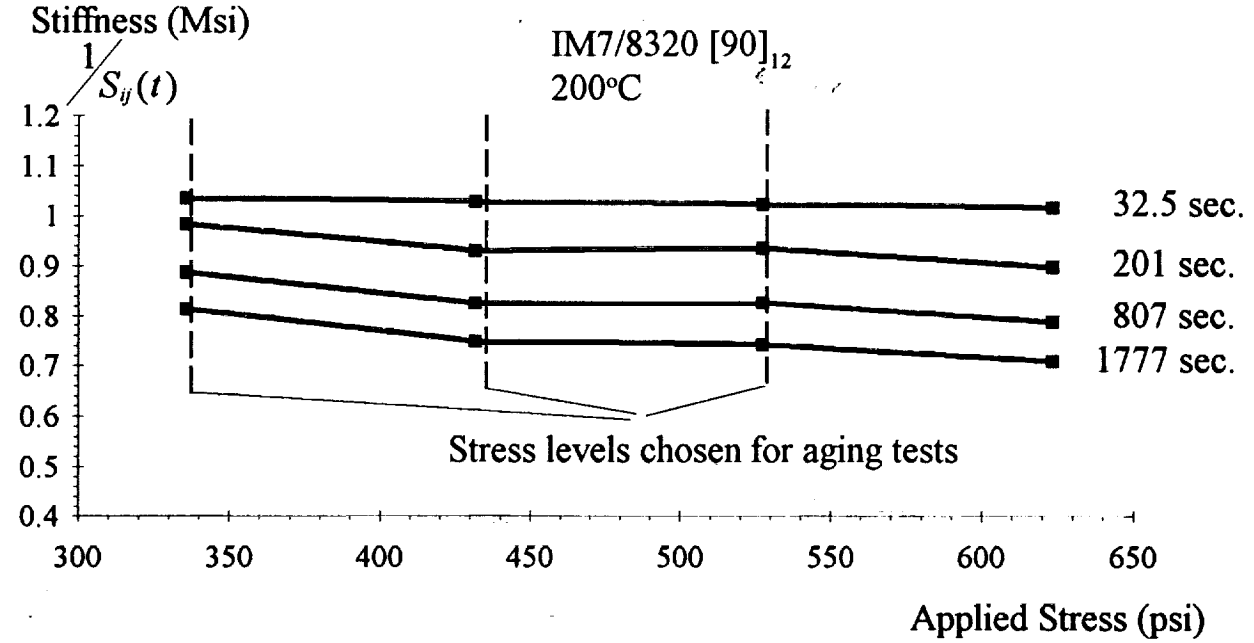

Figure 6. Proportionality check using creep data of transverse specimens tested at 200°C.

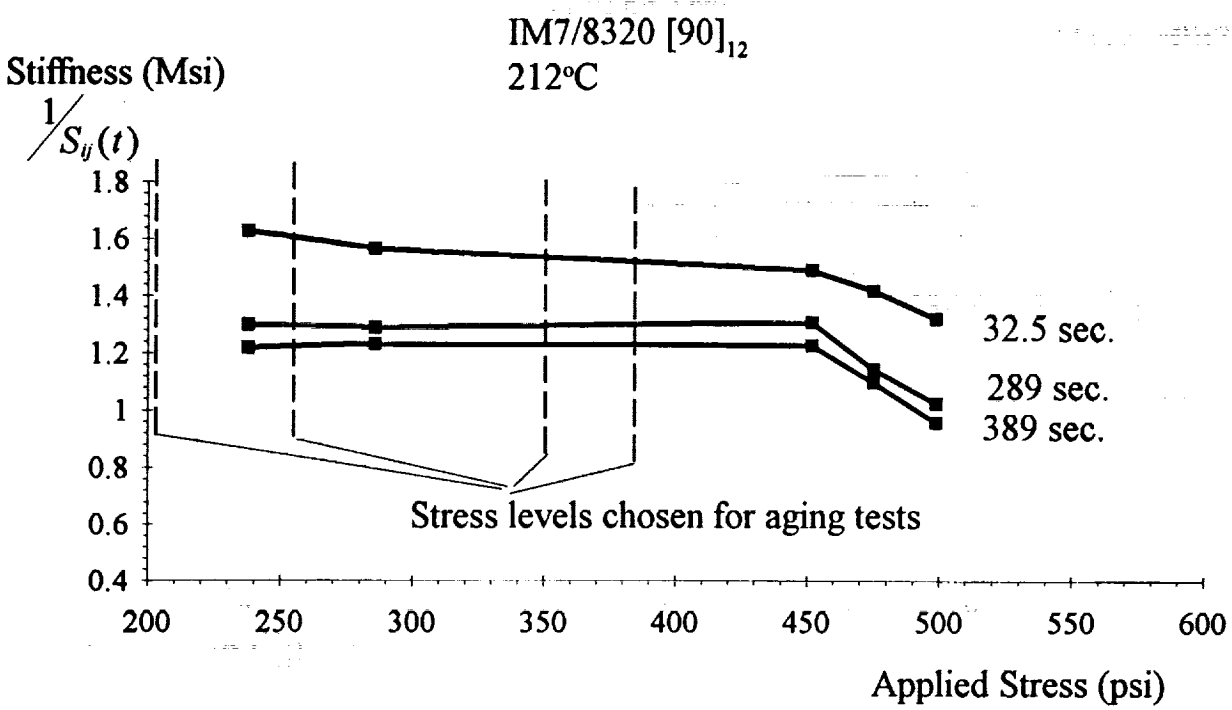

Figure 7. Proportionality check using creep data of transverse specimens tested at 212°C.

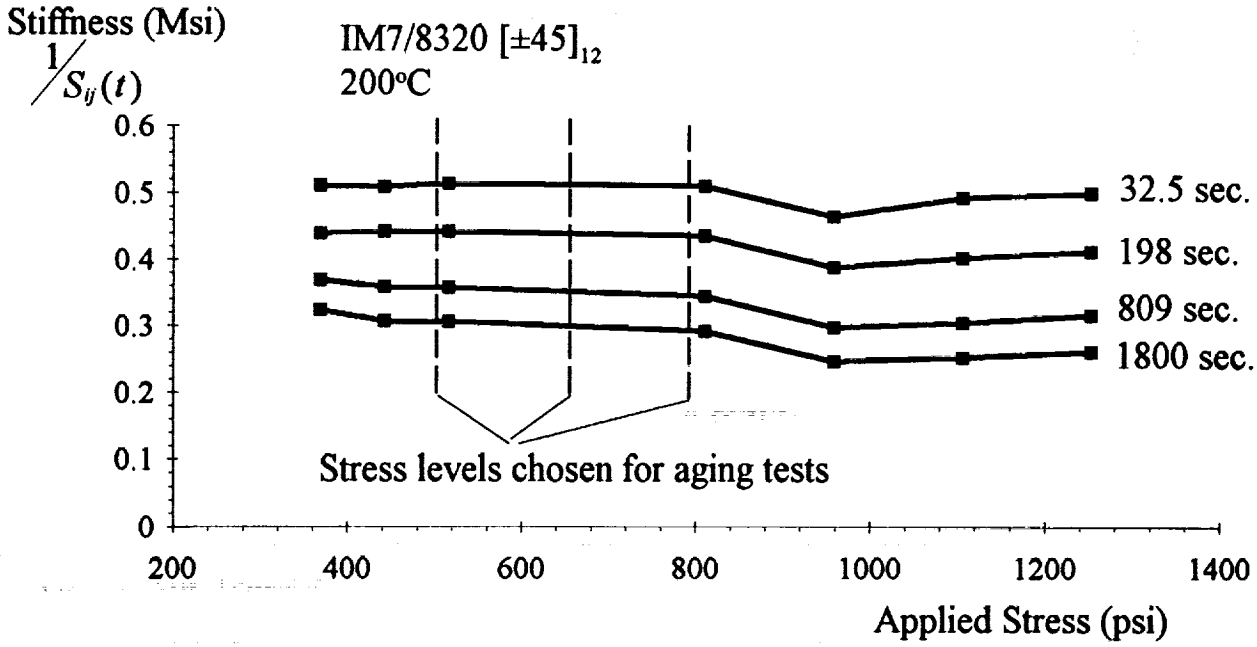

Figure 8. Proportionality check using creep data of shear specimens tested at 200°C.

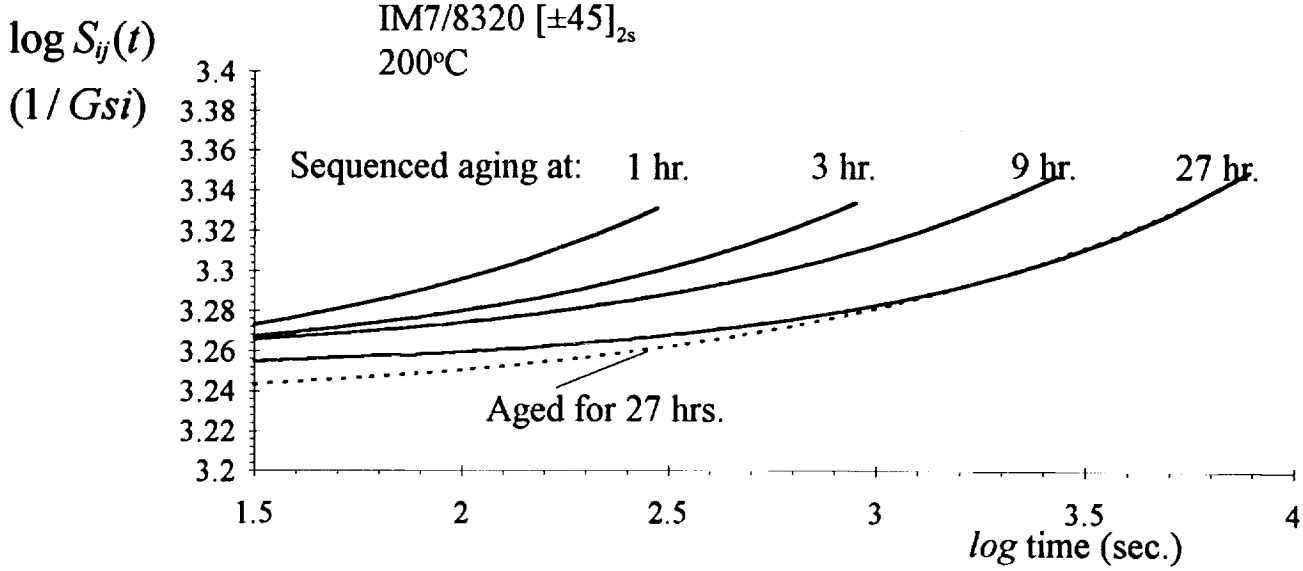

Figure 9. Comparison of sequenced versus unsequenced creep compliance test data.

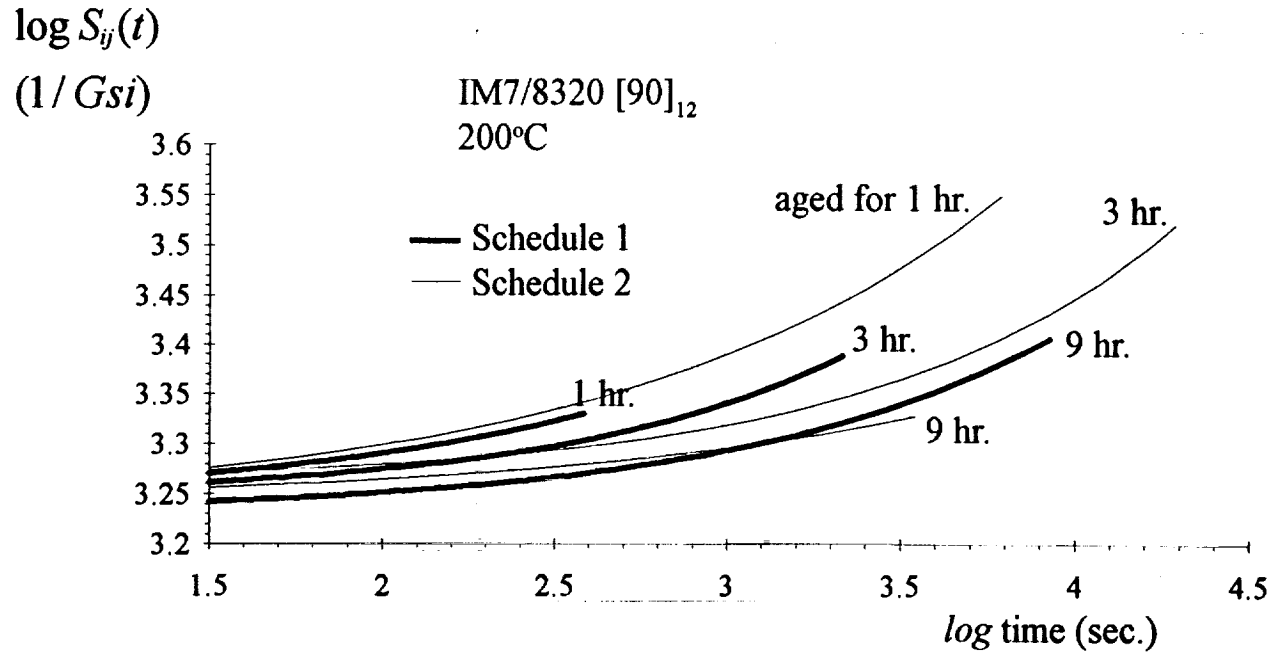

Figure 10. Test data showing the effects of extended load periods during sequenced creep compliance testing

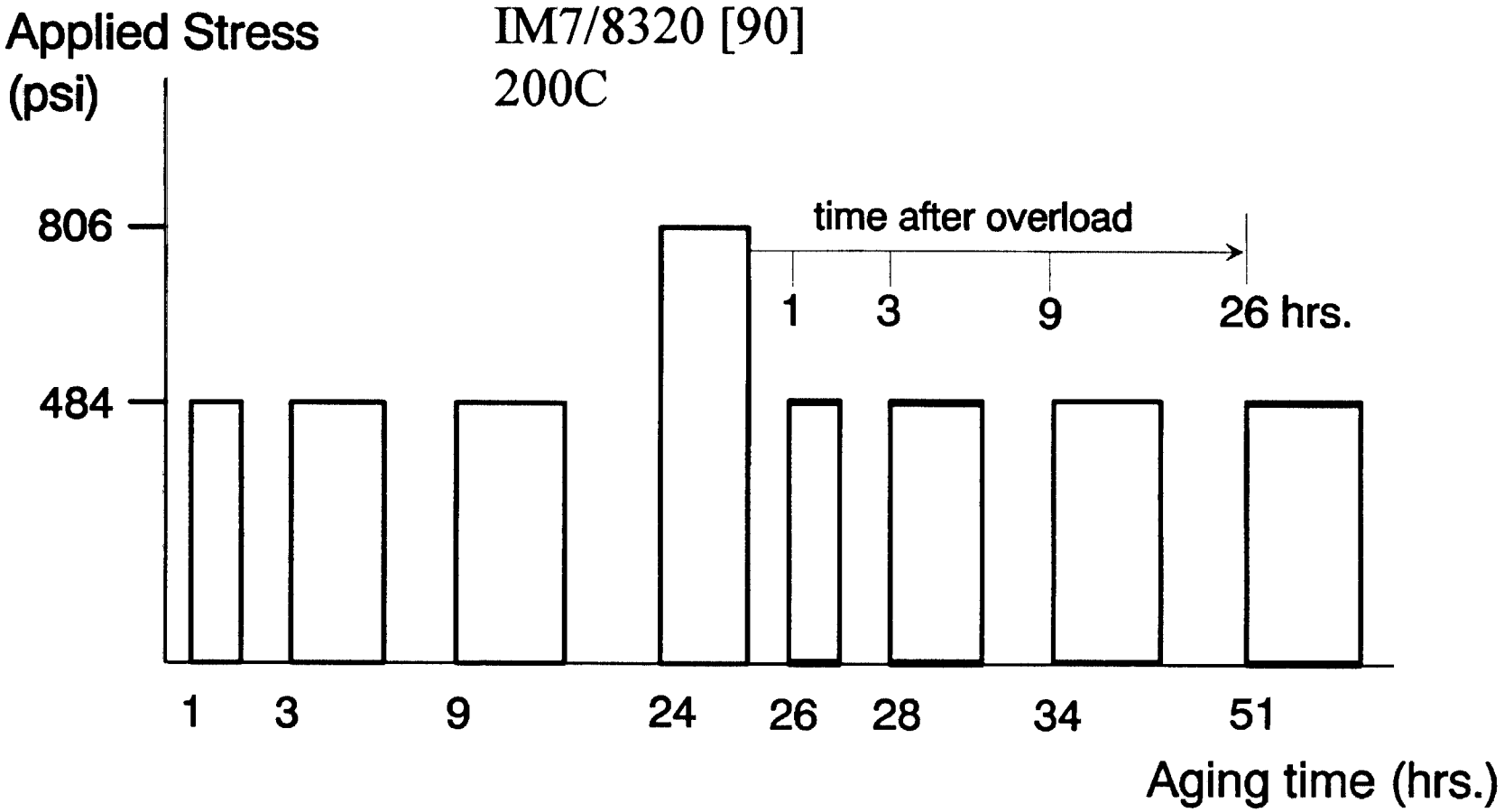

Figure 11. Loading schedule for the stress overload test.

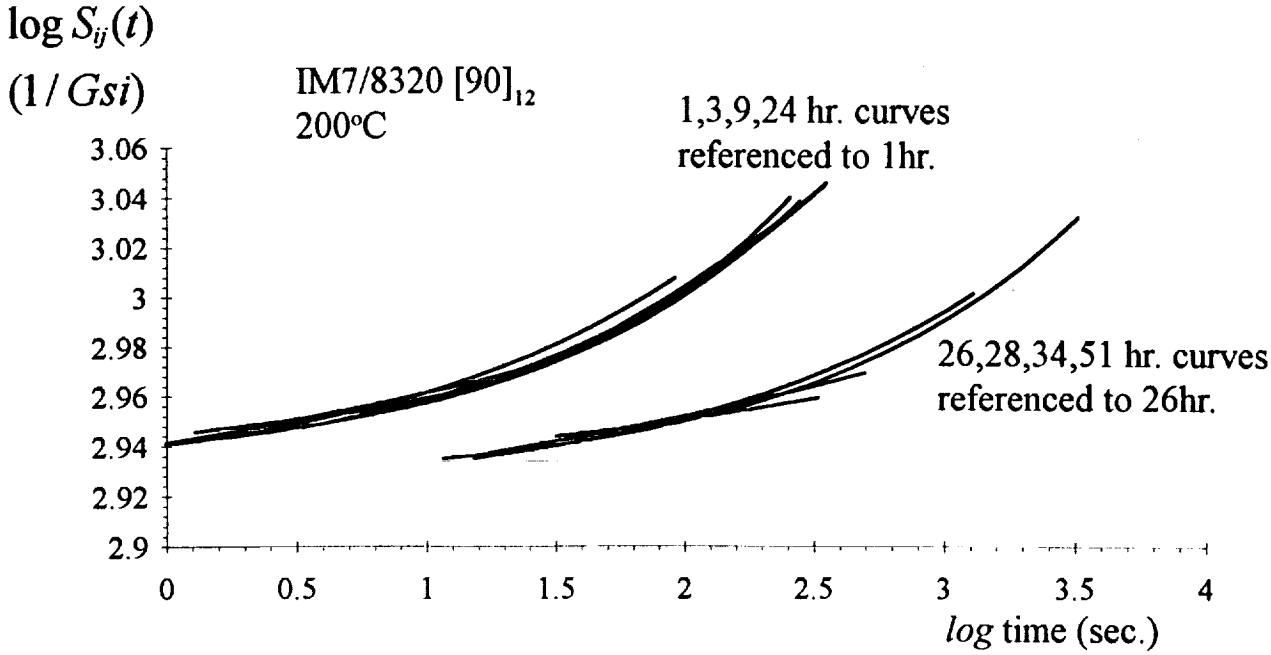

Figure 12a. Measured creep compliance curves prior to and after a stress overload.

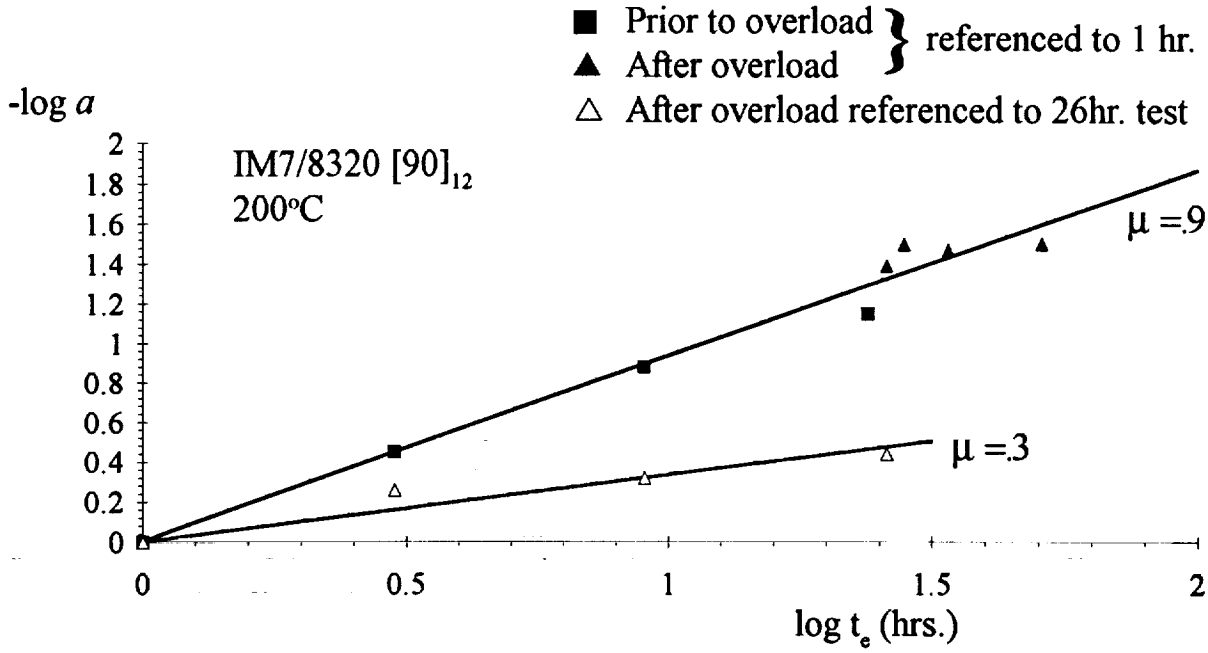

Figure 12b. Measured aging shift factors prior to and after a stress overload.

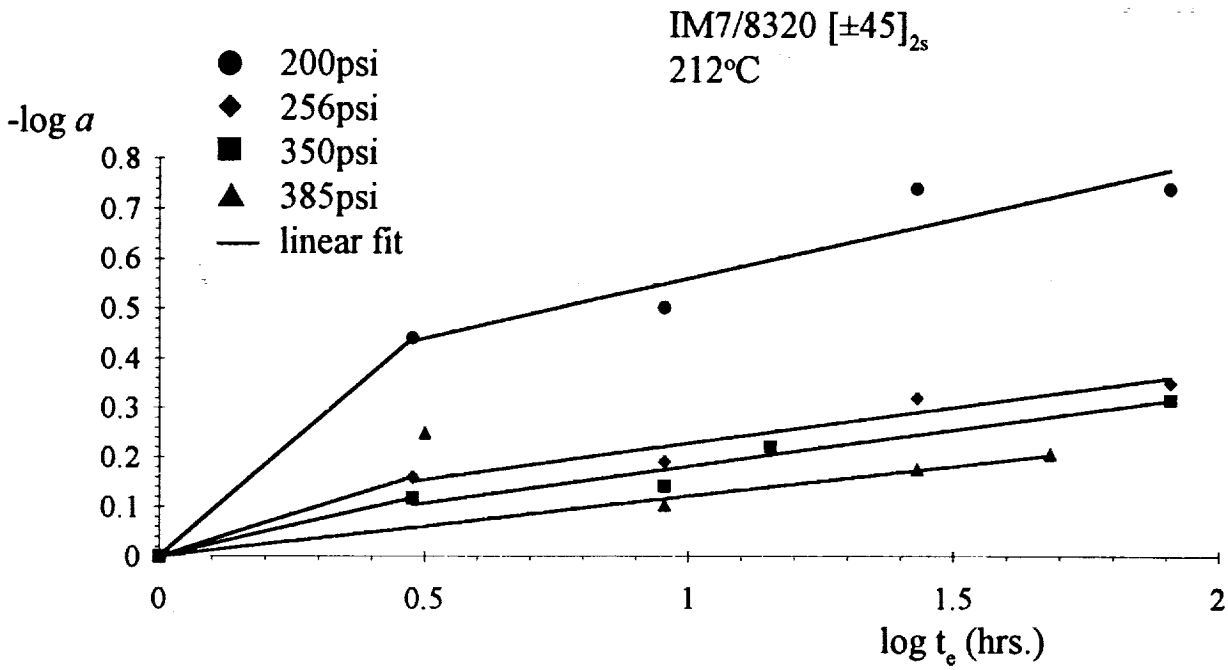

Figure 13. Measured shift factors from an aging to equilibrium test, found using horizontal (time) shifts only.

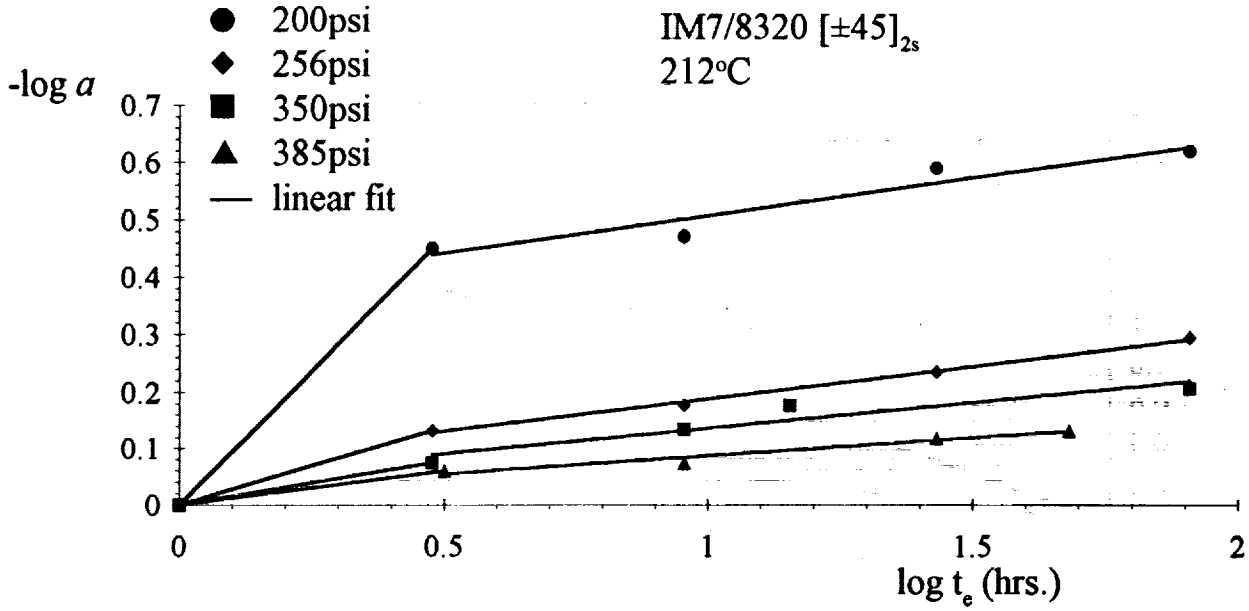

Figure 14. Measured shift factors from an aging to equilibrium test, found using horizontal (time) and vertical (compliance) shifts.

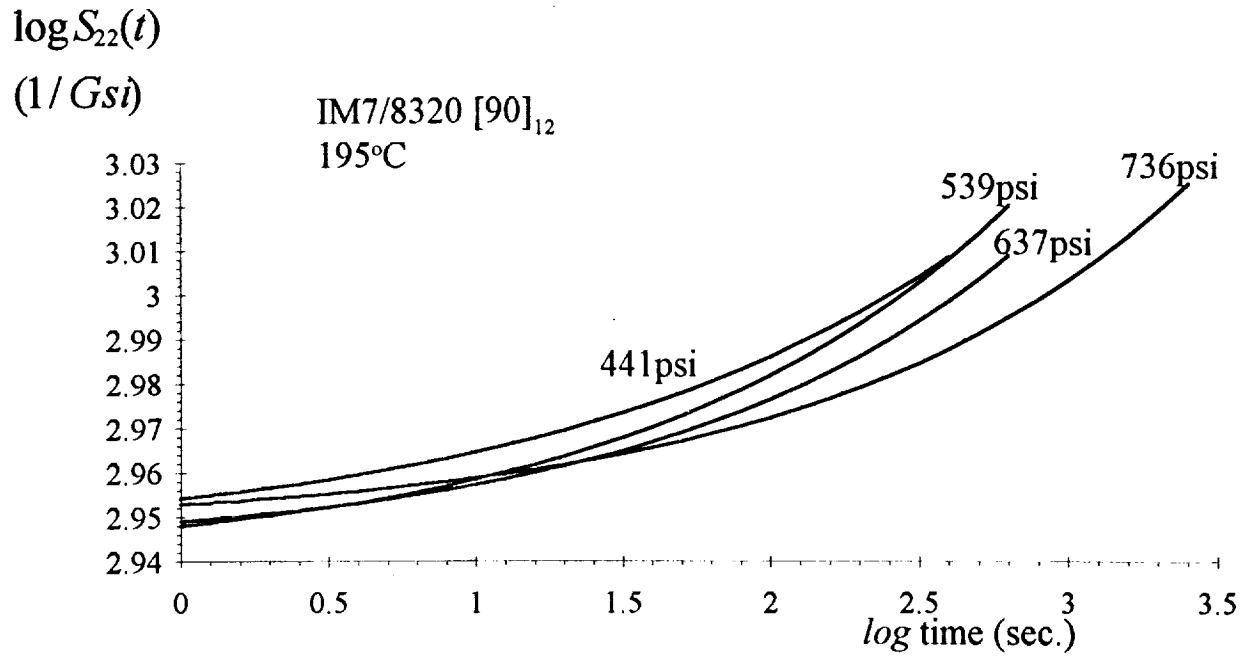

Figure 15. Momentary master curves for a transverse specimen at 195°C and various applied stress levels.

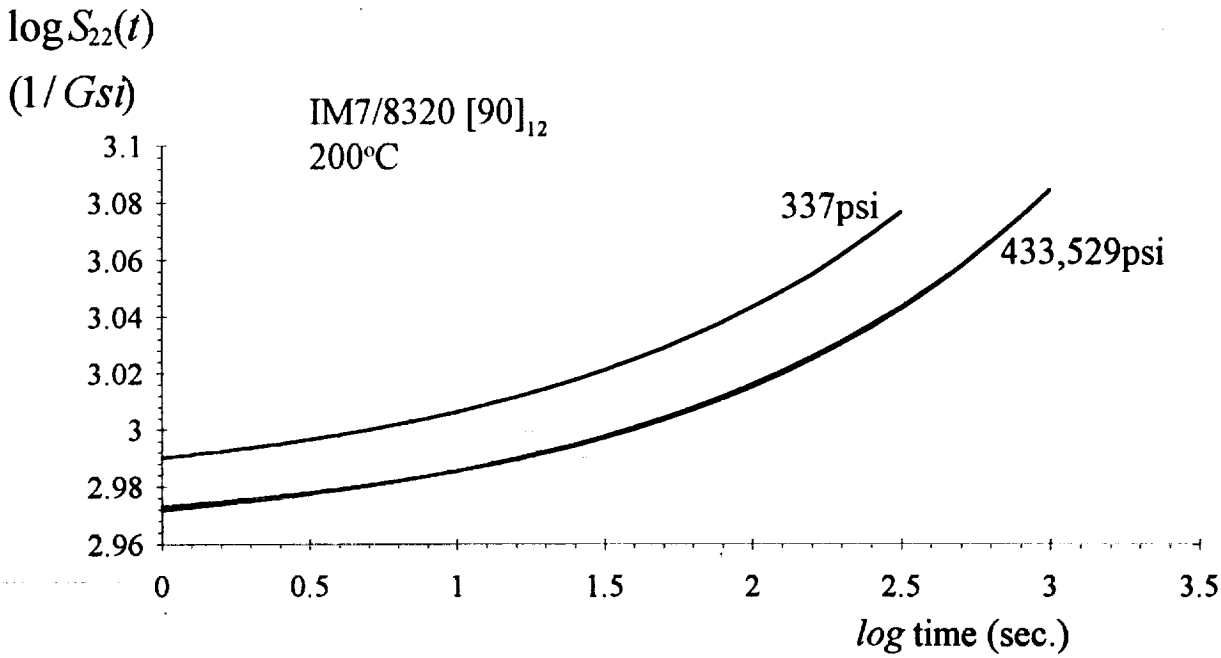

Figure 16. Momentary master curves for a transverse specimen at 200°C and various applied stress levels.

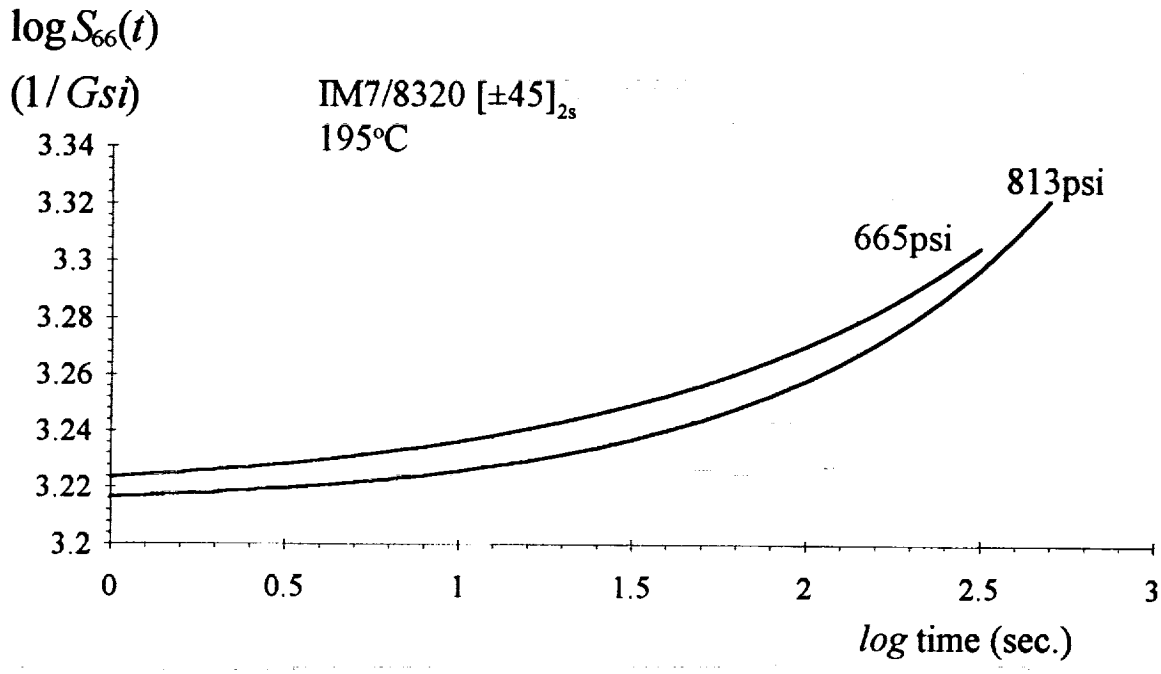

Figure 17. Momentary master curves for a shear specimen at 195°C and various applied stress levels.

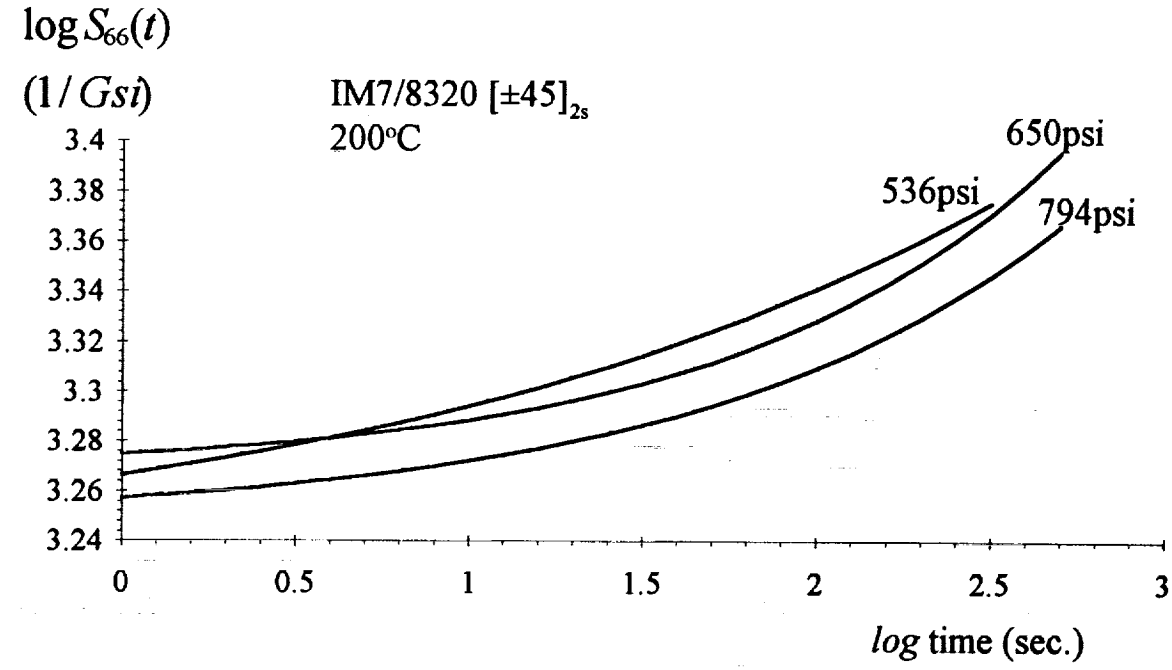

Figure 18. Momentary master curves for a shear specimen at 200°C and various applied stress levels.

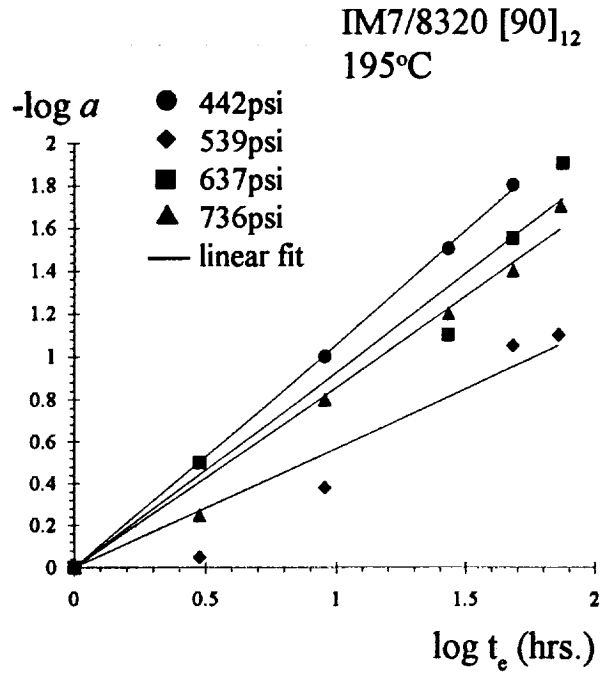

Figure 19. Measured aging shift factors for transverse specimens at 195°C and various stress levels.

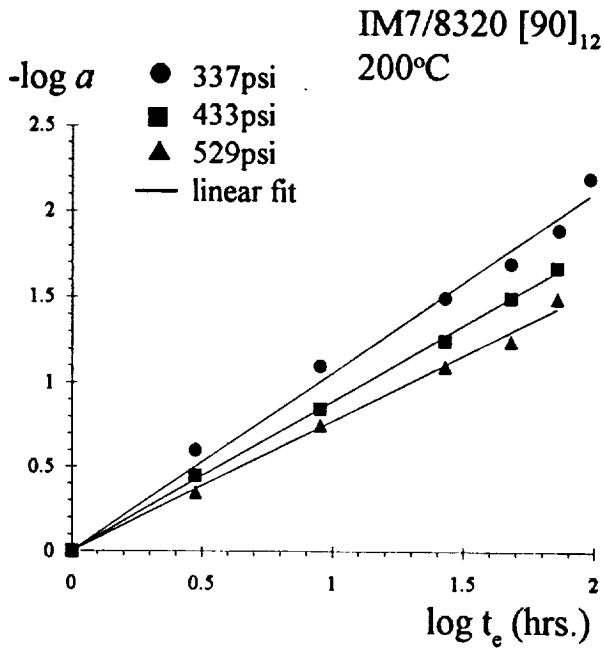

Figure 20. Measured aging shift factors for transverse specimens at 200°C and various stress levels.

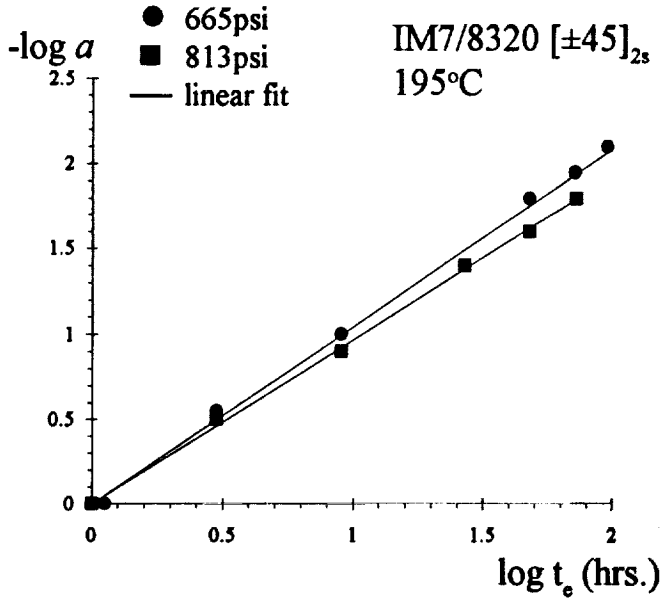

Figure 21. Measured aging shift factors for shear specimens at 195°C and various stress levels.

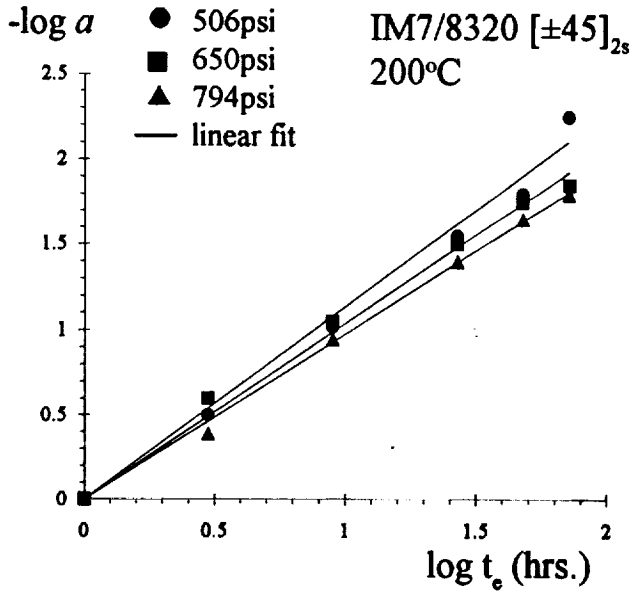

Figure 22. Measured aging shift factors for shear specimens at 200°C and various stress levels.

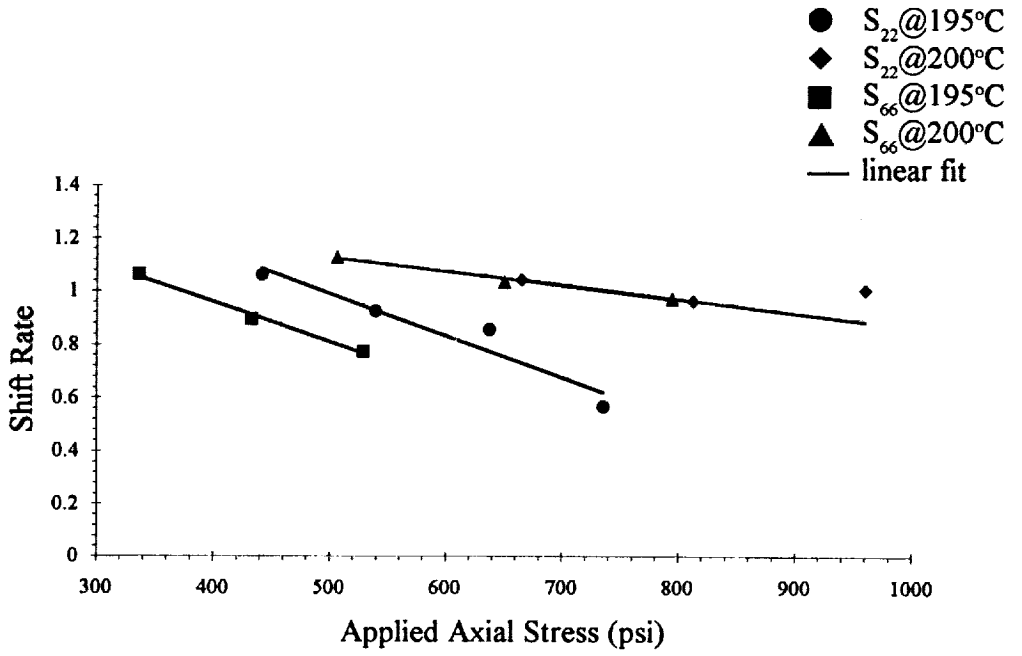

Figure 23. Measured aging shift rates for all tests versus the applied stress.

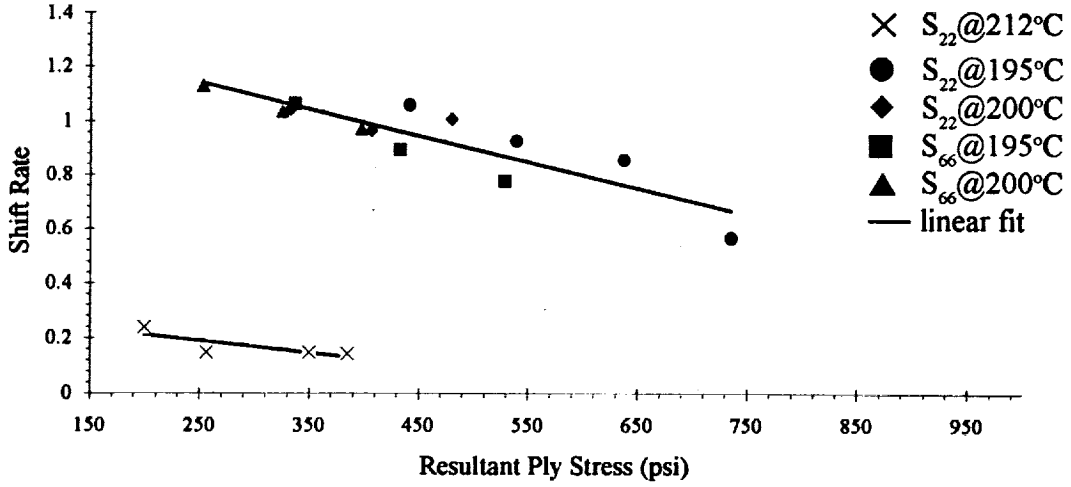

Figure 24. Measured aging shift rates for all tests versus the resultant ply stress.

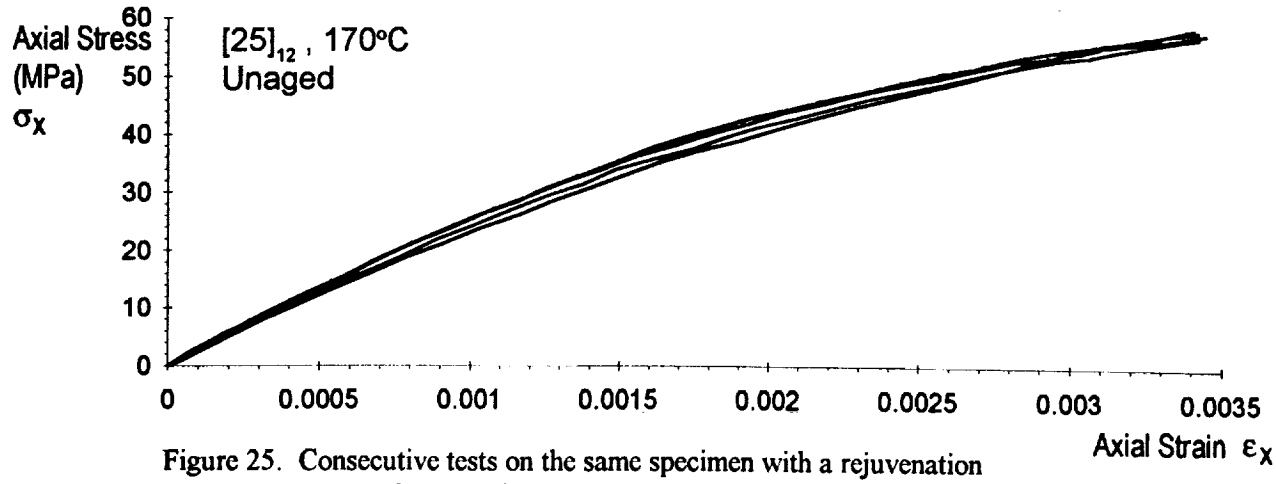

Figure 25. Consecutive tests on the same specimen with a rejuvenation sequence prior to each test.

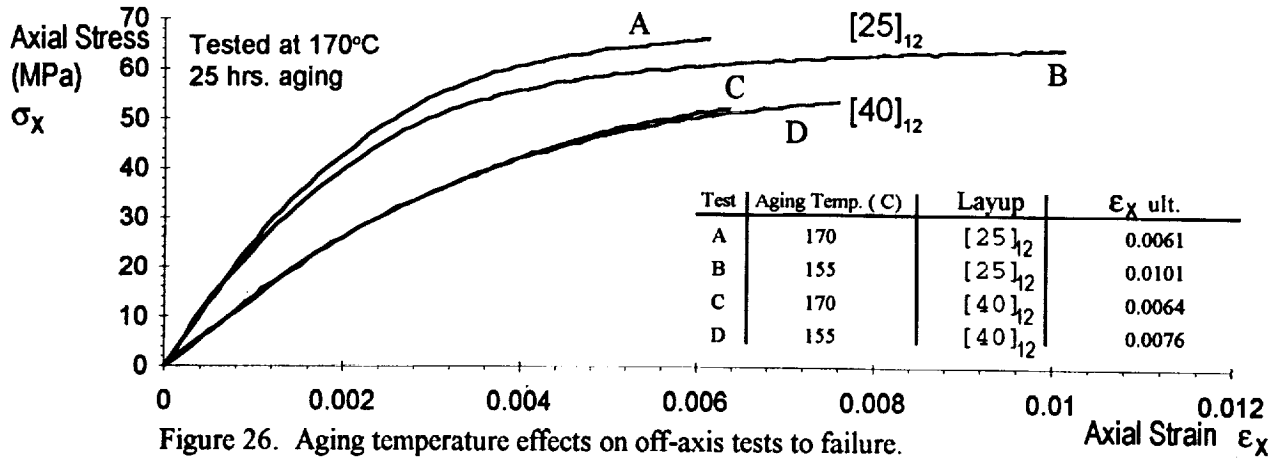

Test	Aging Temp. (C)	Layup	ε_x ult.
A	170	$[25]_{12}$	0.0061
B	155	$[25]_{12}$	0.0101
C	170	$[40]_{12}$	0.0064
D	155	$[40]_{12}$	0.0076

Figure 26. Aging temperature effects on off-axis tests to failure.

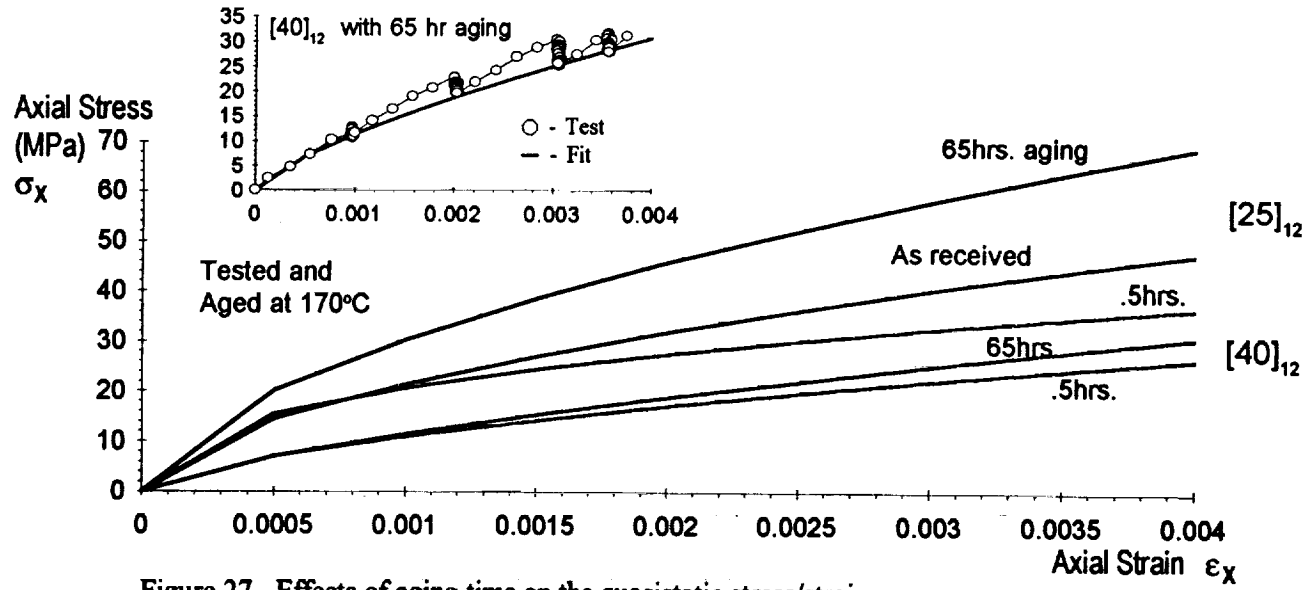

Figure 27. Effects of aging time on the quasistatic stress/strain curves found from the best fit to the relaxation points.

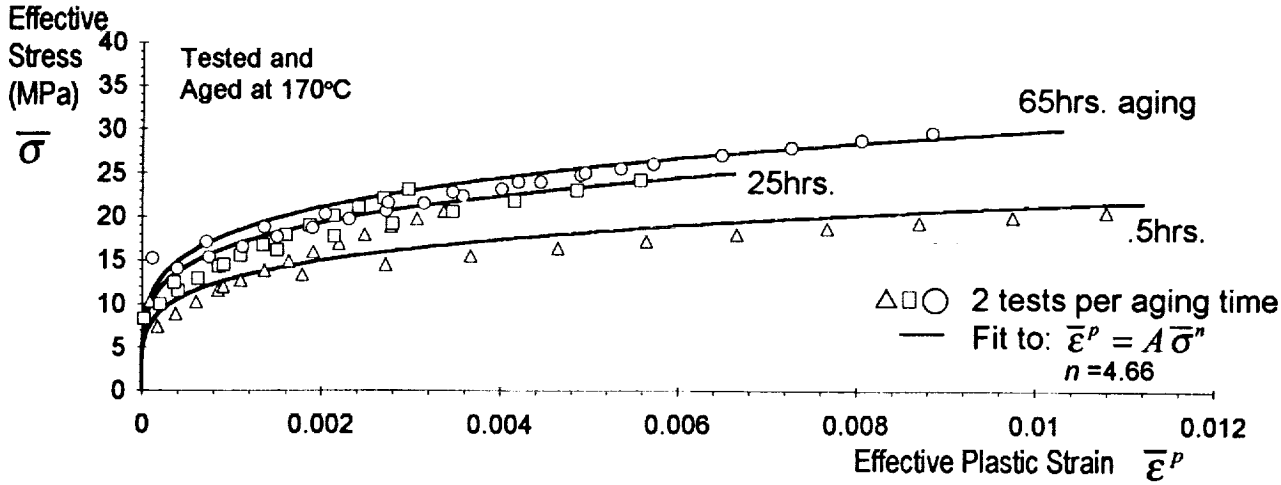

Figure 28. Effects of aging time on the plasticity master curves.

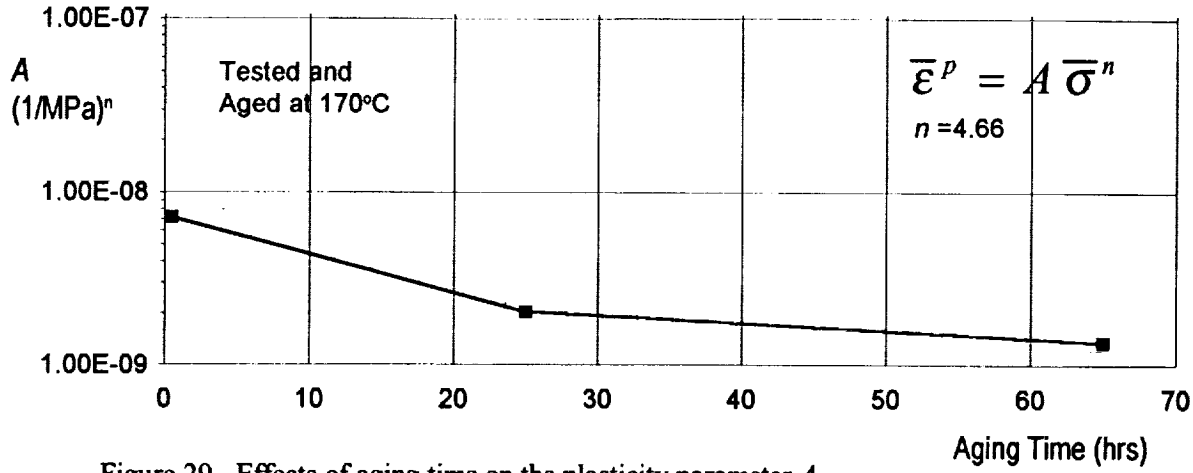

Figure 29. Effects of aging time on the plasticity parameter A.

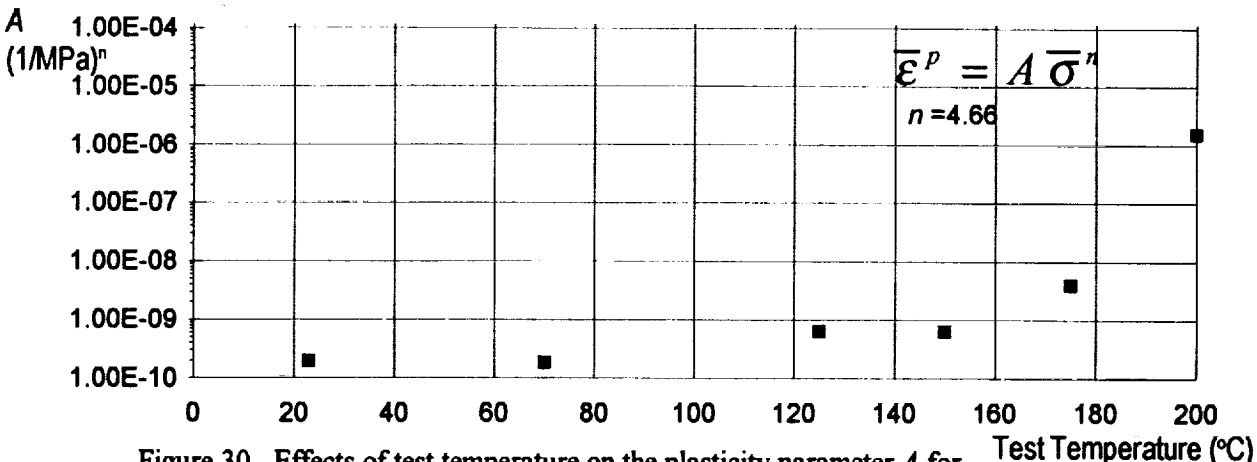

Figure 30. Effects of test temperature on the plasticity parameter A for unaged, as received tests [2].

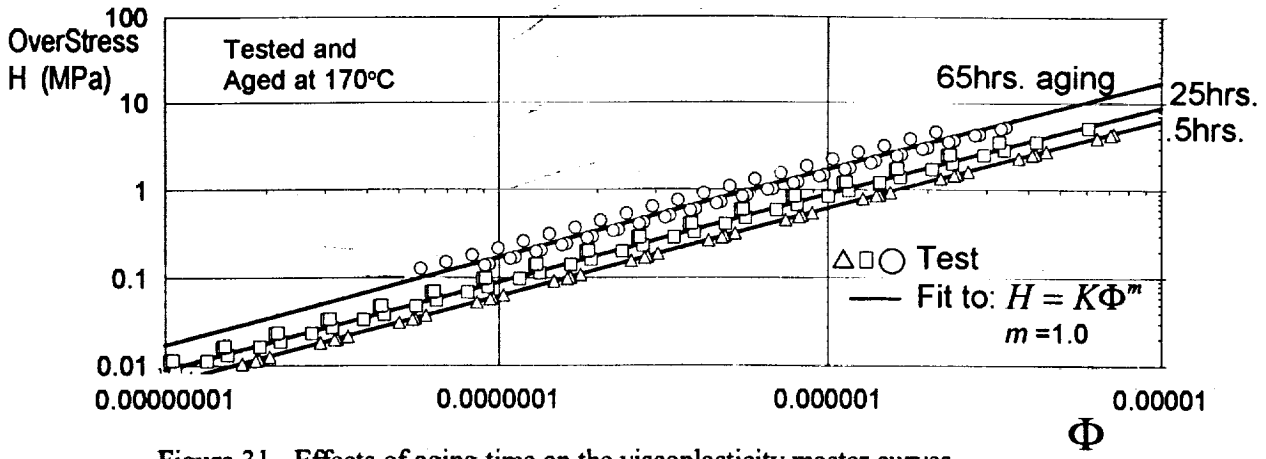

Figure 31. Effects of aging time on the viscoplasticity master curves.

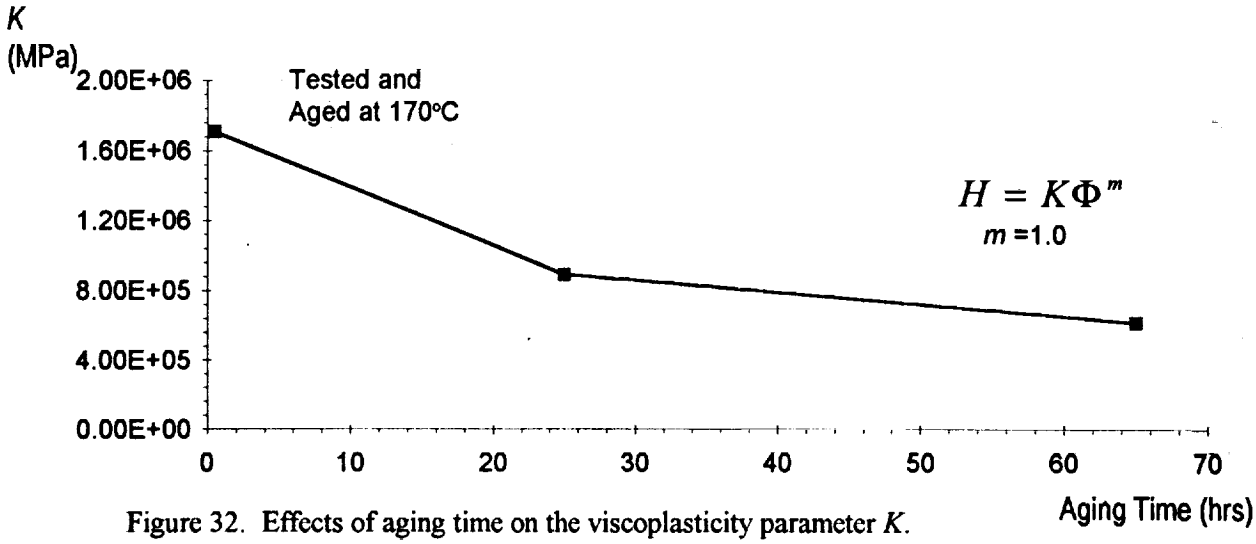

Figure 32. Effects of aging time on the viscoplasticity parameter K.

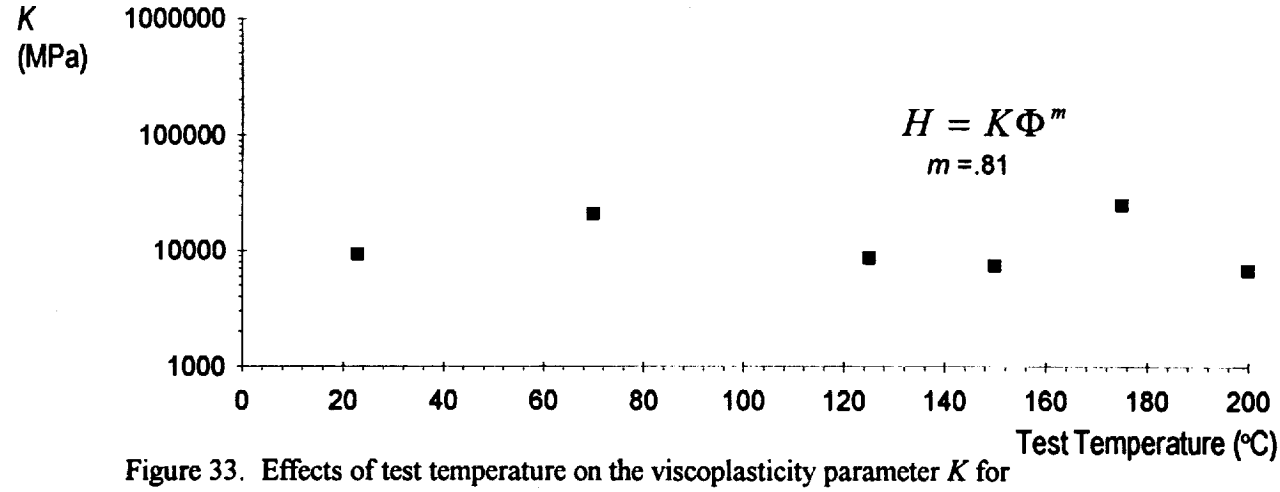

Figure 33. Effects of test temperature on the viscoplasticity parameter K for unaged, as received tests. [2]

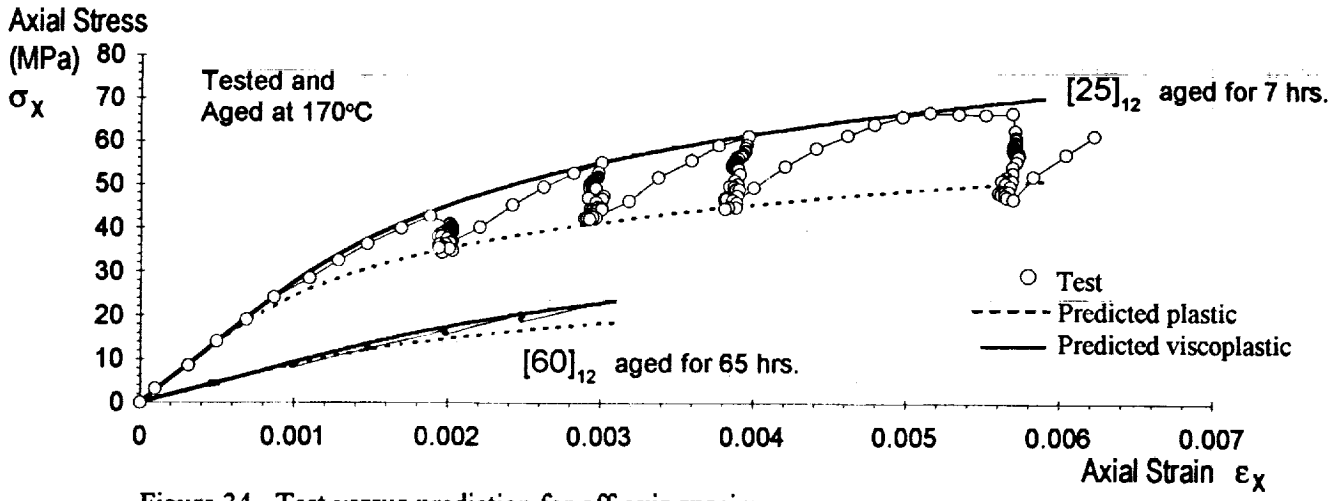

Figure 34. Test versus prediction for off-axis specimens.

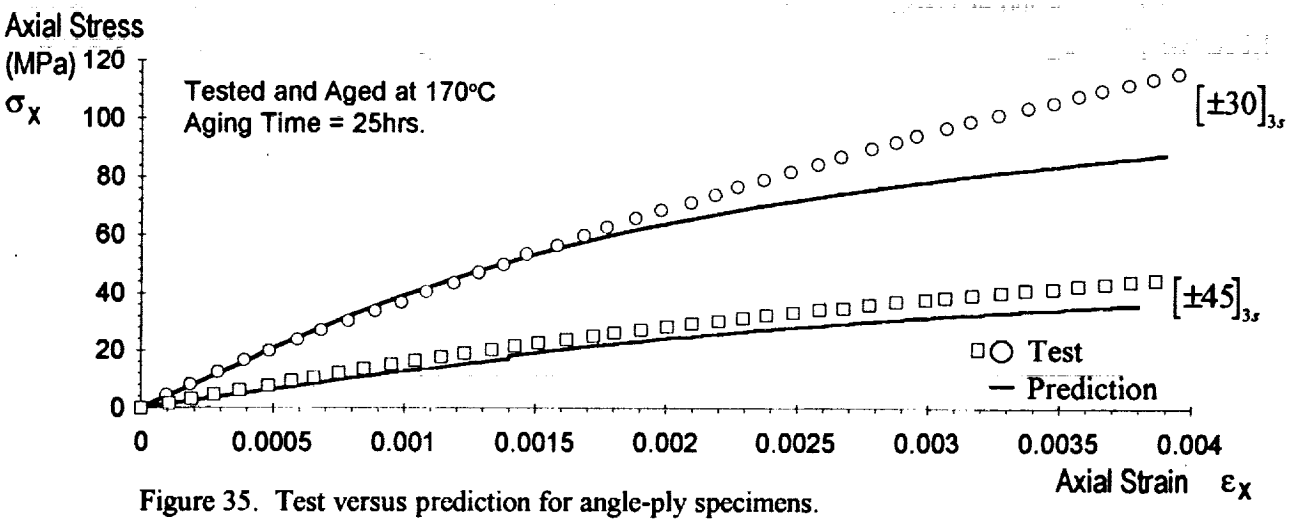

Figure 35. Test versus prediction for angle-ply specimens.

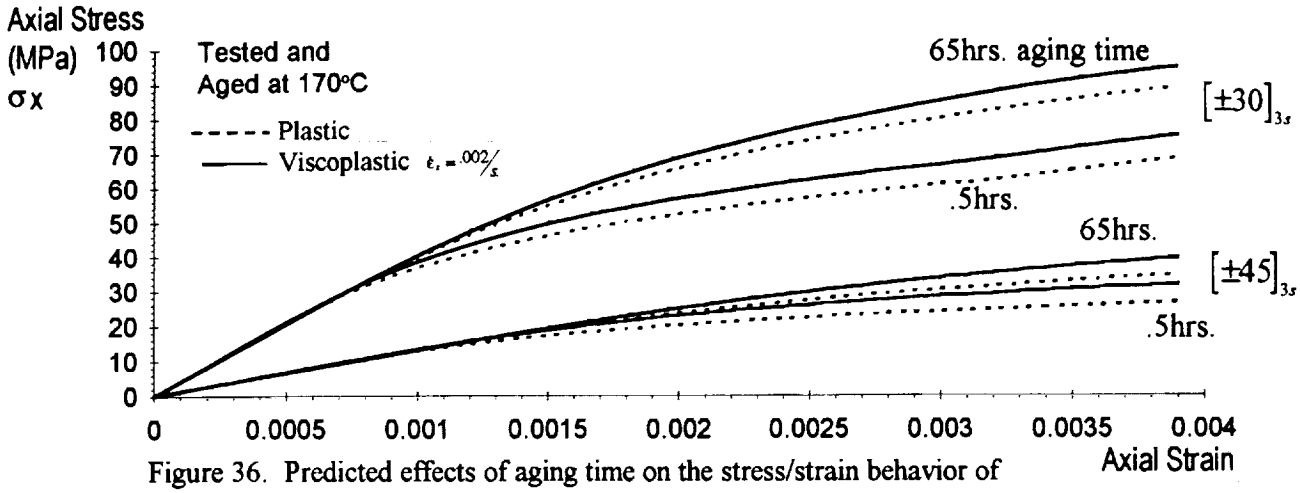

Figure 36. Predicted effects of aging time on the stress/strain behavior of angle-ply specimens.

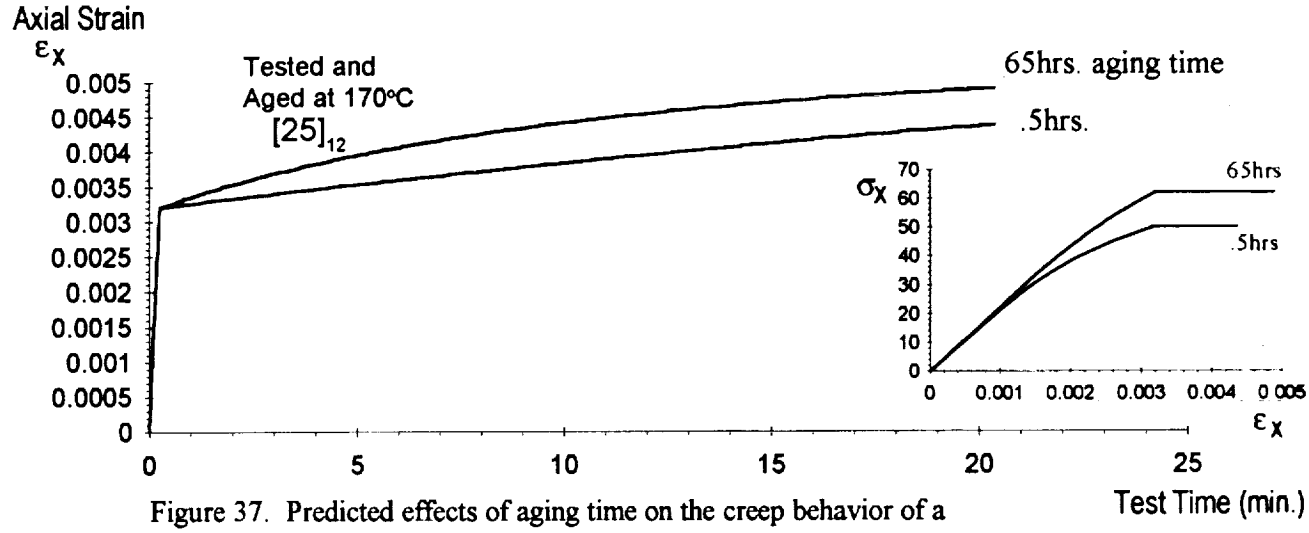

Figure 37. Predicted effects of aging time on the creep behavior of a off-axis specimen.

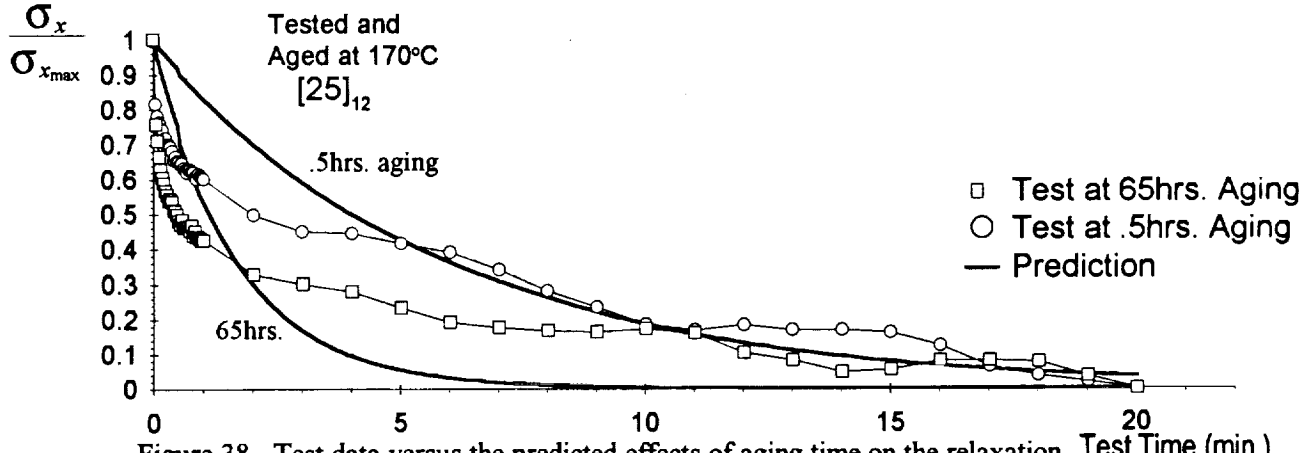

Figure 38. Test data versus the predicted effects of aging time on the relaxation behavior of two off-axis specimens.

REPORT DOCUMENTATION PAGE

Form Approved
OMB No. 0704-0188

1. AGENCY USE ONLY (Leave blank)	2. REPORT DATE	3. REPORT TYPE AND DATES COVERED
	November 1993	Technical Memorandum

4. TITLE AND SUBTITLE

Time Dependent Behavior of a Graphite/Thermoplastic Composite and the Effects of Stress and Physical Aging

5. FUNDING NUMBERS

WU 505-63-50-04

6. AUTHOR(S)

Thomas S. Gates and Mark Feldman

7. PERFORMING ORGANIZATION NAME(S) AND ADDRESS(ES)

NASA Langley Research Center
Hampton, VA 23681-0001

8. PERFORMING ORGANIZATION REPORT NUMBER

9. SPONSORING/MONITORING AGENCY NAME(S) AND ADDRESS(ES)

National Aeronautics and Space Administration
Washington, DC 20546-0001

10. SPONSORING/MONITORING AGENCY REPORT NUMBER

NASA TM 109047

11. SUPPLEMENTARY NOTES

Presented at the AIAA/ASME/ASCE/AHS/ASC 34th SDM Conference, La Jolla, CA, April 19-21, 1993

Gates: Langley Research Center, Hampton, VA; Feldman: Old Dominion University, Norfolk, VA

12a. DISTRIBUTION/AVAILABILITY STATEMENT

Unclassified - Unlimited

Subject Category - 24

12b. DISTRIBUTION CODE

13. ABSTRACT (Maximum 200 words)

Two complimentary studies were performed to determine the effects of stress and physical aging on the matrix dominated time dependent properties of IM7/8320 composite. The first of these studies, experimental in nature, used isothermal tensile creep/aging test techniques developed for polymers and adapted them for testing of the composite material. From these tests, the time dependent transverse (S_{22}) and shear (S_{66}) compliance's for an orthotropic plate were found from short term creep compliance measurements at constant, sub-T_g temperatures. These compliance terms were shown to be affected by physical aging. Aging time shift factors and shift rates were found to be a function of temperature and applied stress.

The second part of the study relied upon isothermal uniaxial tension tests of IM7/8320 to determine the effects of physical aging on the nonlinear material behavior at elevated temperature. An elastic/viscoplastic constitutive model was used to quantify the effects of aging on the rate-independent plastic and rate-dependent viscoplastic response. Sensitivity of the material constants required by the model to aging time were determined for aging times up to 65 hours. Verification of the analytical model indicated that the effects of prior aging on the nonlinear stress/strain/time data of matrix dominated laminates can be predicted.

14. SUBJECT TERMS

Composites; Physical aging; Viscoelasticity; Viscoplasticity; Plasticity

15. NUMBER OF PAGES

40

16. PRICE CODE

A03

17. SECURITY CLASSIFICATION OF REPORT	18. SECURITY CLASSIFICATION OF THIS PAGE	19. SECURITY CLASSIFICATION OF ABSTRACT	20. LIMITATION OF ABSTRACT
Unclassified	Unclassified		